

Task 5b - Flood vulnerability

Regionally consistent risk assessment for earthquakes and floods and selective landslide scenario analysis for strengthening financial resilience and accelerating risk reduction in Central Asia (SFRARR Central Asia disaster risk assessment)

FINAL VERSION

08 December 2022



OGS
National Institute of Oceanography and Applied Geophysics



Akua Capital



**TOSHKENT DAVLAT
TRANSPORT UNIVERSITETI**
Ташкентский государственный
транспортный университет



Revision History

Version	Date	State	Initials	Changes
r1d1	08/10/2021	Draft	RED: GB, GC, SD	
r1d2	15/10/2021	Draft	RED: PB; OGS: SP	General review, copyediting
r1	12/11/2021	Approved	RED: GB	Changes based on reviewers' comments
r2d1	02/12/2021	Draft	RED: GB	Changes based on reviewers' comments
r2	23/12/2021	Approved	RED: GB, PB; OGS: SP	Changes based on reviewers' comments
r3d1	11/01/2022	Draft	RED:GB	Changes based on reviewers' comments
r3	27/01/2022	Approved	RED: GB, PB; OGS: SP	Changes based on reviewers' comments
r5	17/10/2022	Approved	RED: GB, GC, PC	Changes carried out during the calibration process, as part of the activities of Task 6
r6d1	16/11/2022	Draft	RED: GB, GC, PC	Changes based on WB comments
r6	25/11/2022	Approved	RED: GC, PC	Changes based on reviewers' comments. General review, copyediting
	08/12/2022	Approved	WB	

This report takes into account the particular instructions and requirements of our client. It is not intended for and should not be relied upon by any third party and no responsibility is undertaken to any third party.

Technical Assignment number 1266456

RED Risk Engineering + Development

Executive Summary

This report presents the methodological approach for the development of flood vulnerability curves to be used within a flood risk assessment model for five Central Asian countries (Kazakhstan, Kyrgyz Republic, Tajikistan, Turkmenistan and Uzbekistan). This flood risk model is a part of the European Union- and World Bank-funded project called “SFRARR Central Asia disaster risk assessment” (*Regionally consistent risk assessment for earthquakes and floods and selective landslide scenario analysis for strengthening financial resilience and accelerating risk reduction in Central Asia*). In this document, flood vulnerability curves are defined as relationships between a flood intensity measure (the water depth at a given location) and an estimation of the level of damage an asset is subject to, expressed between 0 and 1 (where 0 is no damage and 1 is total damage).

The report is divided into four main sections: buildings, infrastructure, cash crops and population. Buildings include all constructions intended for residential, commercial, industrial or educational purposes. Infrastructure includes roads and railways, airports and dams. Cash crops includes plants cultivated on a large scale for commercial purposes in the target area. Subsistence crops are not considered. Population refers to the human vulnerability, i.e., the possibility that floods might cause loss of life. In each section, the vulnerability of different assets is analysed, from a literature point of view (with especial attention to work previously undertaken in the target area) and from a methodological point of view, and then the resulting vulnerability curves are shown. Details are provided on how the vulnerability curves were developed and on the assumptions behind each of them. Numerical results are not provided here but will be delivered in form of tables together with the present report.

Index

EXECUTIVE SUMMARY..... II

1 INTRODUCTION..... 1

2 TAXONOMY..... 5

3 BUILDING VULNERABILITY 8

 3.1 STATE OF THE ART..... 8

 3.2 METHODOLOGY..... 9

 3.3 RESULTS 20

4 INFRASTRUCTURE VULNERABILITY 26

 4.1 STATE OF THE ART..... 26

 4.2 METHODOLOGY..... 28

 4.3 RESULTS 29

5 CROP VULNERABILITY 31

 5.1 STATE OF THE ART..... 31

 5.2 METHODOLOGY..... 32

 5.3 RESULTS 33

6 HUMAN VULNERABILITY 35

 6.1 STATE OF THE ART..... 35

 6.2 METHODOLOGY..... 35

 6.3 RESULTS 38

7 CONCLUSIONS 41

REFERENCES..... 42

APPENDIX A - LIST OF ACRONYMS..... 45

Index of Figures

Figure 1 – Reclassification of the domain into three geomorphological areas. Green: plains, yellow: hills, brown: mountains. 2

Figure 2 – Methodological conceptualisation of a building-by-building empirical curve (Oliveri and Santoro, 2000). 8

Figure 3 – Scheme of the methodological approach for buildings. 9

Figure 4 – Building types from (Wieland et al., 2015). 13

Figure 5 – Distribution of area of building footprints as derived from the OSM buildings dataset. Areas are in m² (The World Bank, 2017). 16

Figure 6 – Examples of calibrated vs uncalibrated vulnerability curves. 21

Figure 7 – Vulnerability curves for category “RC1: RC (reinforced concrete) frame without ERD” and geomorphological area “plains”. 22

Figure 8 – Vulnerability curves for category “URM1: Unreinforced masonry” and geomorphological area “hills”. 22

Figure 9 – Vulnerability curves for category “WOOD1: Timber structure” and geomorphological area “mountains”. 23

Figure 10 – Vulnerability curves for category “Industrial” and geomorphological area “hills”. 23

Figure 11 – Vulnerability curves for category “URM1: Unreinforced masonry” and geomorphological area. 24

Figure 12 – Vulnerability curves residential, industrial and commercial buildings in Central Asia according to the Global Flood Depth-Damage database (Huizinga et al., 2017). 25

Figure 13 – Damage Scanner (Klijn et al., 2007) vulnerability curves, including infrastructure/road curve (Bubeck et al., 2011; de Moel and Aerts, 2011). 26

Figure 14 – Standard Method vulnerability curves for roads and railways (Kok et al., 2004). 26

Figure 15 – Damage curves for illustrative values of road construction costs, in euros per kilometre (van Ginkel et al., 2021). 27

Figure 16 – Flood vulnerability curves for roads and infrastructure for Asian countries and comparison with the European curve (Huizinga et al., 2017). 27

Figure 17 – Railway damage mechanisms (Kellermann et al., 2015). 28

Figure 18 – Railway vulnerability curves for the Netherlands (de Bruijn et al., 2015) and for other countries (Wang et al., 2021). 28

Figure 19 – Costs of airport components (Scawthorn et al., 2006). Amounts in thousands of dollars. 29

Figure 20 – Vulnerability curve for roads and railways (left) and for airports (right) used in this project (the road and railway curve is taken from the GFDD database, the airport curve is elaborated from GFDD and HAZUS). 30

Figure 21 – Literature flood vulnerability curve for cotton. 32

Figure 22 – Vulnerability curve for cash crops used in this project. 34

Figure 23 – Simplified representation of the human body in a (a) lateral and (b) frontal view (Milanesi et al., 2016). 35

Figure 24 – Flow velocity distributions according to the geomorphological area. 36

Figure 25 – Occupancy and number of floors for buildings in Kyrgyz Republic (Pittore et al., 2011). 37

Figure 26 – Vulnerability curve for human beings used in this project (Kazakhstan). 38
Figure 27 – Flood vulnerability curve for human beings used in this project (Kyrgyz Republic). 39
Figure 28 – Flood vulnerability curve for human beings used in this project (Tajikistan). 39
Figure 29 – Flood vulnerability curve for human beings used in this project (Turkmenistan). 40
Figure 30 – Flood vulnerability curve for human beings used in this project (Uzbekistan). 40

Index of Tables

Table 1. Categorisation of the assets at risk. 2

Table 2. List of partner countries of the consortium and associated scientific institutions 4

Table 3. Summary of the taxonomy for residential buildings. 5

Table 4. Summary of the taxonomy for non-residential buildings. 6

Table 5. Summary of the taxonomy for infrastructure..... 7

Table 6. Damage components considered in the vulnerability model.10

Table 7. Weights of the aggregated variable “number of floors” for each exposure category.12

Table 8. Weights of the aggregated variable “Basement height” for each exposure category.14

Table 9. Weights of the aggregated variable “Ground floor level” for each exposure category.14

Table 10. Weights of the aggregated variable “Building type” for each exposure category.15

Table 11. Unit costs per country.17

Table 12. Flood duration and flow velocity distributions in each geomorphological area (plains have slower velocities and longer durations, mountains have faster velocities and shorter durations)18

Table 13. Studies on flood vulnerability of crops.....31

1 Introduction

This report describes the methodology used for the development of flood vulnerability curves for five Central Asian countries (Kazakhstan, Kyrgyz Republic, Tajikistan, Turkmenistan and Uzbekistan), within the framework of a broader flood risk model being developed in a European Union- and World Bank-funded project called “SFRARR Central Asia disaster risk assessment” (Regionally consistent risk assessment for earthquakes and floods and selective landslide scenario analysis for strengthening financial resilience and accelerating risk reduction in Central Asia). The objective of this task is to develop relationships between a flood intensity measure and an estimation of the level of damage an asset experiences. These relationships, expressed between 0 and 1 (where 0 is no damage and 1 is total damage, which, for the purpose of the present model, is intended as the total reconstruction cost), are called the vulnerability curves and sometimes damage curves or damage functions.

In this flood risk model, the sole intensity measure used to assess damage by flood is the water depth and therefore the vulnerability curves developed here are always expressed in terms of water depth vs damage ratio (i.e., the level of damage, between 0 and 1). Water depth is widely considered as the intensity measure with the highest correlation with the flood damage (Kreibich et al., 2009). However, other variables may play a role in the determination of the damage caused by a flood, such as duration, current velocity, deposits, contamination by pollution and salinity of water. While these variables cannot be considered explicitly in the present risk model due to the large extension of the geographical domain and the complexity/resolution of the hazard model, the vulnerability curves developed in this study do take into account some of these ancillary intensity measures indirectly, as a secondary modifier or in a statistical manner. In particular, the local slope has been used as a proxy for the flow velocity and the flood duration. The geographical domain of the model has been reclassified into three geomorphological areas:

- Plains: where the terrain slope is less or equal to 1%;
- Hills: where the terrain slope is larger than 1% and less or equal to 15%;
- Mountains: where the terrain slope is larger than 15%.

Vulnerability curves for each category asset at risk have been differentiated based on where the asset is located (i.e., on plains, hills or mountains), accounting indirectly for the effect of flow velocity and flood duration. The slope has been calculated based on the 90m digital elevation model MERIT-Hydro (Yamazaki et al., 2019). The resulting map can be seen in Figure 1.

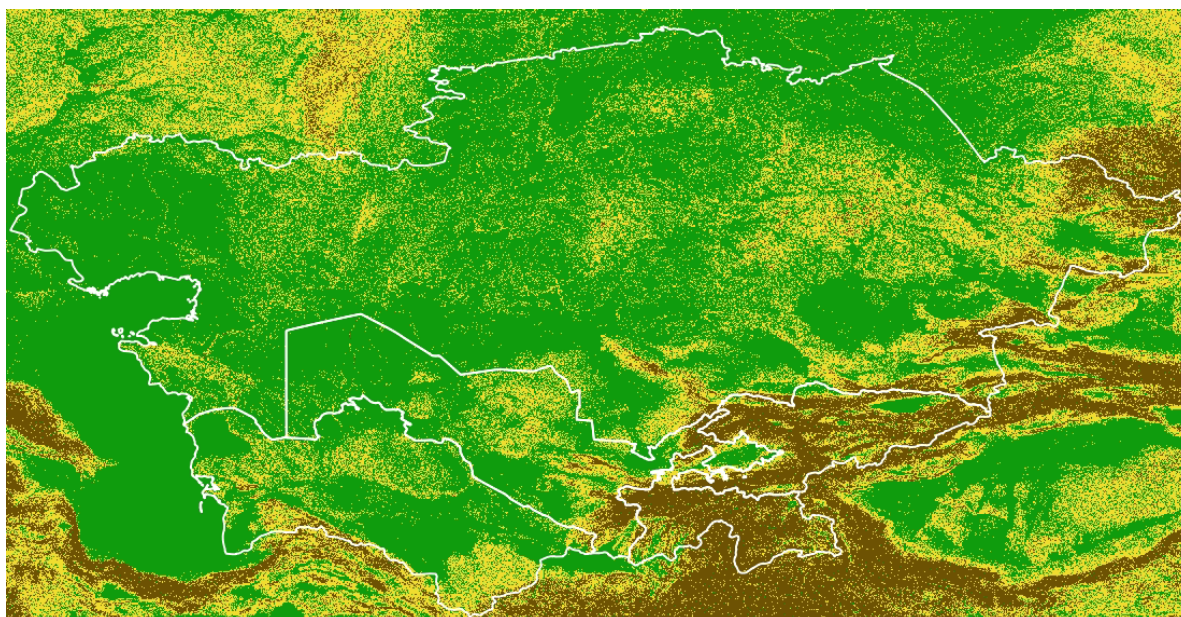


Figure 1 – Reclassification of the domain into three geomorphological areas. Green: plains, yellow: hills, brown: mountains.

The assets subject to flood risk, and for which flood vulnerability should be assessed, are grouped into four categories (buildings, infrastructure, crops and population) and are defined in the following table (Table 1). More information regarding the definition of the asset classes can be found in the specific exposure characterisation report (developed within the project as part of Task 4 – Development of an exposure dataset). For the residential buildings, the code names taken from Pittore et al. (2020) are reported.

Table 1. Categorisation of the assets at risk.

Category	Class description	Code name from Pittore et al. (2020)	Taxonomy (present project)
Buildings	Residential - Unreinforced masonry	URM1	/MUR + CLBRS + MOC/LWAL + DNO/FW + HBET:2,4 + YBET/1930,1960
	Residential - Unreinforced masonry concrete floors	URM2	MUR+ MOCL/LWAL + DNO/FC + HBET:1,2 + YBET/1930,1960
	Residential - Confined masonry	CM	/MCF + MOC/LWAL + DNO/FC/HBET:1,5 + YBET/1960,2001
	Residential - Reinforced masonry, low rise	RM-L	/MR + MOC/LWAL + DNO/FC/HBET:1,1 + YBET:1960,2001
	Residential - Reinforced masonry, medium rise	RM-M	/MR + MOC/LWAL + DNO/FC/HBET:3,4 + YBET:1960,2001
	Residential - Reinforced concrete frame without earthquake-resistant design	RC1	/CR + CIP/LFM + DUC/FC/HBET:3,7 + YBET:1957,2006
	Residential - Reinforced concrete frame with moderate earthquake-resistant design	RC2	/CR + CIP/LDUAL + DNO/FC/HBET:4,9 + YBET:1957,2020

Category	Class description	Code name from Pittore et al. (2020)	Taxonomy (present project)
	Residential - Reinforced concrete frame with high level of earthquake-resistant design	RC3	/CR + CIP/LFINF + DNO/FC/HBET:2,5 + YBET:1957,2021
	Residential - Reinforced concrete walls without earthquake-resistant design	RC4	/CR + CIP/LWAL + DNO/FC/HBET:4,16 + YBET:1957,2006
	Residential - Reinforced concrete walls with moderate level of earthquake-resistant design	RCPC1	/CR + PC/LWAL + DUC/FC/HBET:1,16 + ybet:1956,1980
	Residential - Reinforced concrete) walls with high level of earthquake-resistant design	RCPC2	/CR + PC/LFLS + DUC/FC/HBET:3,12 + YBET:1980,2020
	Residential - Adobe	ADO	/MUR + ADO/LWAL + DNO/FW/HBET:1
	Residential - Timber structure	WOOD1	/W/LWAL + DUC/FW/HBET:1,2 + YPRE:2021
	Residential - Timber structure	WOOD2	/W+ WLI/LO + DUC/FW/HBET:1
	Residential - Steel structure	STEEL	/S/LFM + DNO/FME/HBET:1
	Residential - Other structure	OTH	UNK+HBET:1
	Schools	-	UNK + YBET:1960,2021
	Hospitals	-	UNK + HBET:1,16 + YBET:1956,2021 UNK/ + HBET:1,5 + YBET:1930,2021
	Commercial	-	UNK/ + HBET:1,6 UNK/ + HBET:1,5 + YBET:1930,2021
	Industrial	-	IND_UNK+HBET:1:2 EN/O EN/GAS EN/SOL EN/OIL EN/HYD PWG PWR COM
Infrastructure	Roads - motorways	-	RDN+MO
	Roads - primary	-	RDN+TR RDN+PR
	Roads - secondary	-	RDN+SE RDN+TE
	Railways	-	RLW+LR RLW+MR RLW+RL
	Airports	-	AIR
	Dams	-	DAM
Crops	Cotton	-	CRP9+5
	Wheat	-	CRP1+1
	Other crops	-	-
Population	Adult, male	-	-
	Adult, female	-	-
	Elderly, male	-	-

Category	Class description	Code name from Pittore et al. (2020)	Taxonomy (present project)
	Elderly, female	-	-
	Child, male	-	-
	Child, female	-	-

When possible and when data support such a decision, vulnerability functions have been differentiated by country (for example, for each category of the residential buildings, five curves have been derived, one for each of the five target countries). It must also be mentioned that the five curves corresponding to the class “dams” are always zero, i.e., dams are considered not vulnerable to flood for the purposes of this study.

All the vulnerability curves presented in this report are defined as relationships between the water depth (intensity measure) and the fraction of total replacement cost (damage ratio).

The development of a regional model cannot be done without the contribution of experts from the local scientific community. Partnership with local governmental institutions and authorities is also an essential step to facilitate model acceptance and for potential integration with national models. Following this concept, the consortium has engaged with the local communities for building and extending awareness of risk and for enhancing the technical capacity of local experts in the use of open tools and resources (see Table 2 for the complete list of involved scientific institutions from each partner country). Institutions and consultants based in all five countries are part of the consortium, and, as such, are involved in all aspects of the project development. Table 2 shows the list of involved institutions and their main representatives. Each institution has made a team available to the consortium. For most of the tasks required for the development of flood vulnerability, these local partners have provided their knowledge and expertise and advised on matters related to specific characteristics of their respective countries. In cases where the experience of the local partners needed to be integrated with knowledge from other professional figures, engagement with such figures has been undertaken by the local partners, who have looked for the right persons and interacted with them. As an example, data on unit repair and removal costs were retrieved also thanks to interactions with local architects and engineers who were not in the team of the consortium but were sought out and interviewed by the local partners.

Table 2. List of partner countries of the consortium and associated scientific institutions

Country	Main Scientific Institution	Local Representative
Kazakhstan	IS - Institute of Seismology under MoES of RoK	Dr. Natalya Silacheva
Kyrgyz Republic	ISNASKR - Institute of Seismology, National Academy of Sciences, Kyrgyz Republic	Prof. Kanatbek Abdrakhmatov
Tajikistan	IWPHE - Institute of Water Problems, Hydropower Engineering and Ecology	Prof. Zainalobudin Kobuliev
Turkmenistan	Various individual consultants	Dr. Japar Karaev
Uzbekistan	ISASUz - Institute of Seismology, Academy of Sciences, Uzbekistan	Prof. Vakhitkhan Ismailov

2 Taxonomy

This section describes the residential, non-residential and infrastructure taxonomy classification for the central Asian countries. The residential building typology consists of six main building types with a total of 15 subtypes (Table 3) following the strategies described by Wieland et al., (2015) and more recently by Pittore et al. (2020). The taxonomy is defined according to the GED4ALL mapping scheme. Herein we do not go through details of the definition of the classes and the parameters in the current document. More information about the definition of the acronyms used in the following tables can be found in the exposure modelling reports of this project (see report of Task 4 – Exposure data development). Several different surveys have been conducted in the Kyrgyz Republic and in Tajikistan between 2012 and 2016, for a total of around 7000 buildings remotely surveyed. The surveys have been conducted by local engineers experienced in the local building practices. The surveyed buildings are then mapped to the building type. These typologies are deemed to be representative of the building stock in the region, in different proportions according to the country and the type of settlement (e.g., urban or rural). Non-residential buildings include eight different occupancy types as listed in Table 4. Table 5 shows the fractions of different building classes for the non-residential buildings. We also consider ten classes of infrastructure for road, railways and bridges. Table 5 shows and describes these classes.

Table 3. Summary of the taxonomy for residential buildings.

No	EMCA macro-typology	EMCA sub-class	Description	Taxonomy
1	EMCA1	URM1	Unreinforced masonry	/MUR + CLBRS + MOC/LWAL + DNO/FW + HBET:2,4 + YBET/1930,1960
2		URM2	Unreinforced masonry concrete floors	MUR+ MOCL/LWAL + DNO/FC + HBET:1,2 + YBET/1930,1960
3		CM	Confined masonry	/MCF + MOC/LWAL + DNO/FC/HBET:1,5 + YBET/1960,2001
4		RM-L	Reinforced masonry, low rise	/MR + MOC/LWAL + DNO/FC/HBET:1,1 + YBET:1960,2001
5		RM-M	Reinforced masonry, medium rise	/MR + MOC/LWAL + DNO/FC/HBET:3,4 + YBET:1960,2001
6	EMCA2	RC1	RC (reinforced concrete) frame without ERD	/CR + CIP/LFM + DUC/FC/HBET:3,7 + YBET:1957,2006
7		RC2	RC (reinforced concrete) frame with moderate ERD	/CR + CIP/LDUAL + DNO/FC/HBET:4,9 + YBET:1957,2020
8		RC3	RC (reinforced concrete) frame with high level of ERD	/CR + CIP/LFINF + DNO/FC/HBET:2,5 + YBET:1957,2021
9		RC4	RC (reinforced concrete) walls without ERD	/CR + CIP/LWAL + DNO/FC/HBET:4,16 + YBET:1957,2006
10	EMCA3	RCPC1	RC (reinforced concrete) walls with moderate level of ERD	/CR + PC/LWAL + DUC/FC/HBET:1,16 + ybet:1956,1980

11		RCPC2	RC (reinforced concrete) walls with high level of ERD	/CR + PC/LFLS + DUC/FC/HBET:3,12 + YBET:1980,2020
12	EMCA4	ADO	Adobe	/MUR + ADO/LWAL + DNO/FW/HBET:1
13	EMCA5	WOOD1	Timber structure, load-bearing braced frames	/W/LWAL + DUC/FW/HBET:1,2 + YPRE:2021
14		WOOD2	Timber structure, wooden frame and mud infill	/W+ WLI/LO + DUC/FW/HBET:1
15	EMCA6	STEEL	Steel structure	/S/LFM +DNO/FME/HBET:1

Table 4. Summary of the taxonomy for non-residential buildings.

Building type	Taxonomy	Description	Material fractions
Industrial	IND_UNK+HBET:1:2	Defined as the weighted combination of the most common industrial taxonomies in post-soviet countries (see metadata for details)	31% EMCA1,25% EMCA2, 7% EMCA3, 4% EMCA5, 33% EMCA6
Commercial wholesale and services	UNK/ + HBET:1,6	Commercial wholesale and services – Defined as weighted combination of the most common commercial taxonomies in post-soviet countries (see metadata for details)	26% EMCA1, 37% EMCA2, 1% EMCA3, 36% EMCA5,
Commercial retail	UNK/ + HBET:1,5 + YBET:1930,2021	Commercial retail – Defined as the weighted combination of the most common residential taxonomies in each country (see metadata for details)	KAZ: 26%EMCA1, 35% EMCA4, 28% EMCA5, 9% EMCA6 KYR: 31%EMCA1, 67% EMCA4, TAJ: 25% EMCA1, 72%EMCA4 UZB: TUR: 35% EMCA1, 57% EMCA4
Hospitals	UNK + HBET:1,16 + YBET:1956,2021	Hospitals – Defined as the weighted combination of EMCA2 and EMCA3 typologies	50% EMCA2, 50%EMCA3
Clinics	UNK/ + HBET:1,5 + YBET:1930,2021	Clinics – Defined as weighted combination of most common residential taxonomies in each country (see metadata for details)	KAZ: 26%EMCA1, 35% EMCA4, 28% EMCA5, 9% EMCA6 KYR: 31%EMCA1, 67% EMCA4, TAJ: 25% EMCA1, 72%EMCA4 UZB: TUR: 35% EMCA1, 57% EMCA4
	UNK/ + HBET:1,5 + YBET:1930,2021	Other healthcare facilities (dentist, doctor, pharmacy) –	KAZ: 26%EMCA1, 35% EMCA4, 28% EMCA5, 9% EMCA6

Other healthcare facilities		Defined as weighted combination of most common residential taxonomies in each country (see metadata for details)	KYR: 31%EMCA1, 67% EMCA4, TAJ: 25% EMCA1, 72%EMCA4 UZB: N.A TUR: 35% EMCA1, 57% EMCA4
Urban schools	SCHOOL_URB_UNK + YBET:1960,2021	Urban schools – Defined as the weighted combination of most common urban school types in Central Asia	10% EMCA3, 90%URM (31% EMCA4 and the remaining EMCA1)
Rural schools	SCHOOL_RUR_UNK + YBET:1960,2021	Rural schools – Defined as the weighted combination of most common rural school types in Central Asia	22% EMCA3, 78% URM (22% EMCA4 and the remaining EMCA1)

Table 5. Summary of the taxonomy for infrastructure.

Type	Taxonomy	Description
Road network	RDN+MO	Motorway: restricted access major divided highway (i.e., freeway), normally with 2 or more running lanes plus emergency hard shoulder
	RDN+TR	Trunk: the most important roads in a country's system that aren't motorways (not necessarily be a divided highway)
	RDN+PR	Primary: the next most important roads in a country's system (often link larger towns)
	RDN+SE	Secondary: the next most important roads in a country's system (often link towns)
	RDN+TE	Tertiary: the next most important roads in a country's system (often link smaller towns and villages)
Railway network	RLW+LR	Light rail: a higher-standard tram system, normally in its own right-of-way. Often reaches a considerable length (tens of kilometer)
	RLW+MR	Monorail: a single-rail railway
	RLW+RL	Rail: full sized passenger or freight trains in the standard gauge for the country or state
Bridges	RDN+BR	Road bridges: most of them constituted by RC and steel, more than 85% constructed between 1960 and 1990
	RLW+BR	Railway bridges: large majority constituted of RC, most of them with length<25m

3 Building vulnerability

3.1 State of the art

Three flood vulnerability methodological frameworks currently exist in the literature:

- 1 Building-by-building empirical curves. These curves are developed based on highly-detailed studies on target buildings, estimating the damage corresponding to different water depths (plaster, finishing, floors, doors, appliances, systems, etc. - Figure 2). This methodology requires very detailed post-event surveys on representative target buildings. Water level data also needs to be collected at different stages of the flood event. This methodology is very accurate but requires empirical studies that are unfeasible at the scale of this project.

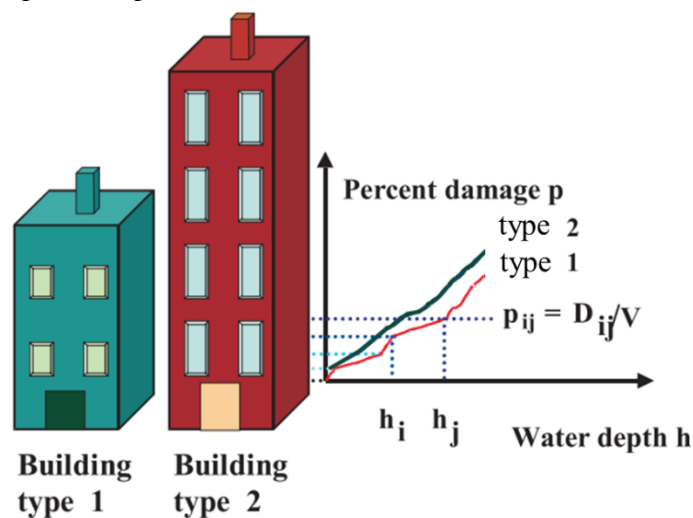


Figure 2 – Methodological conceptualisation of a building-by-building empirical curve (Oliveri and Santoro, 2000).

- 2 Observed damage fitting. In this case, observed economic losses from insurance claims in different buildings are collected, the corresponding water depths are inferred from models or recorded based on visual evidence, and curves are fitted on the water depth vs damage pairs (Luino et al., 2009). This methodology requires post-event surveys, in which damage data is collected, including an assessment of damaged components such as painting, partitions, electrical and plumbing systems, doors, windows, etc. Water level data also needs to be collected if possible (e.g., if water marks are left on the buildings), or, alternatively, a high-resolution flood model needs to be implemented to estimate water depths. This methodology has the advantage of being closely linked to actual economic losses, whose reproduction is the primary objective of a risk model, but requires a large amount of insurance claims data, which are not available in the target countries.
- 3 Component-based flood vulnerability models. These models account for different measures of the event intensity (water depth, but also flow velocity, flood duration, sediment load, water quality, etc.) and different components of the building (structural, non-structural, finishing, doors/windows, systems, basement, etc.) to derive a large set of curves for each component of the damage, which are combined together depending on the characteristics of the building categories (Dottori et al., 2016). This methodology is

particularly suited for regional or large-scale studies as it can be automatized, it is highly flexible and it can provide different levels of accuracy depending on the input data.

Aside from the methodological framework, it is worth mentioning that open flood vulnerability curves datasets for different classes of buildings exist in the literature. A notable example is the Global Flood Depth-Damage dataset developed by the European Union’s Joint Research Centre (Huizinga et al., 2017). These curves have the advantage of being immediately available, but they are defined on very generic building typologies. Also, they are not specifically tailored for the five target countries. All vulnerability curves should ideally be validated with real-world damage data, which in general is very scarce. This is particularly true for component-based curves but also for “bulk” curves such as the Global Flood Depth-Damage dataset. However, the former ones have the advantage of being physically-based (i.e., they consider the actual damage mechanisms and the cost of each component), while the second ones are often derived as the average of several existing curves and might lose their physical meaning along the averaging process.

3.2 Methodology

No specific flood vulnerability curves for buildings developed for the five target countries exist in the literature to the authors’ knowledge, and, for this reason, new curves have been developed within the frame of the present project. A component-based flood vulnerability model, called INSYDE, has been used to develop vulnerability curves (Dottori et al., 2016). A scheme of the methodology is provided in Figure 3.

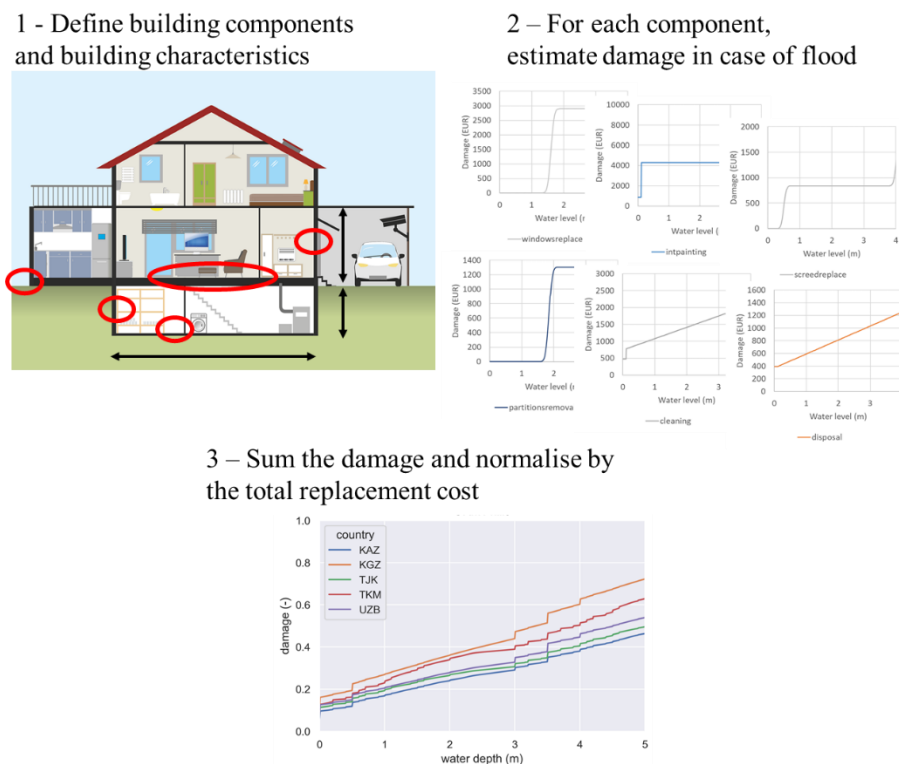


Figure 3 – Scheme of the methodological approach for buildings.

The model accounts for the damage components shown in Table 6.

Table 6. Damage components considered in the vulnerability model.

Category	Component
Clean-up	pumping water out of a basement/house
	removing and disposing debris and mud from a basement/house
	deep cleaning a house after a flood
	extracting humidity from walls and floors after a flood
Removal	removal of the screed
	removal of the wooden floor
	removal of the pavement/floor
	removal of the baseboard
	removal of internal walls/partitions
	removal of plasterboard
	removal of the external plaster
	removal of the internal plaster
	removal of the doors
	removal of the windows
removal of boiler	
Non-structural	construction of walls/internal partitions
	laying down the screed
	setting plasterboard
Structural	soil consolidation works
	local structural repair
	pillar retrofitting
Finishing	setting external plaster
	setting internal plaster
	external painting
	internal painting
	setting of the pavement
	replacing the baseboard
Windows and doors	replacement of doors
	replacement of windows
Building systems	replacement of the heating system
	painting the radiators
	replacement of the floor heating system
	replacement of the electrical system
	replacement of the plumbing system

For each of these components a vulnerability curve was derived based on simple geometrical and logical criteria. For example, in the case of the component “Pumping”, the cost for water pumping for a generic building is calculated by considering water volumes stored in the basement (if at all present in the building) and in the part of building below the street level (if any).

$$ext = IA \cdot (-GL) + BA \cdot (-BL)$$

$$C = up \cdot ext$$

where:

ext is the extension of the building component to be removed/replaced (in this case, in m³)

IA is the internal area of the building (m²)

GL is the ground floor height below the street level (m)

BA is the basement area (m²)

BL is the basement level below the street level (m)

C is the damage (in EUR)

up is the unit price for the removal/replacement of the building component (in this case, in EUR/m³).

In this specific case, the damage does not depend on the water depth, because it is considered to be an on/off damage, i.e., it only depends on whether the building has been flooded or not (i.e., if the building has been flooded, all areas below street level are considered flooded and water has to be pumped out).

In other cases, the damage depends on the water level and thus is computed for different water levels (from 0.05 m to 5 m). An example is "Internal painting".

$$ext = IP * N * IH + BP * BH$$

$$C = up \cdot ext$$

Where:

ext is the extension of the building component to be removed/replaced (in this case, in m²)

IP is the internal perimeter of the building (m)

N is the number of flooded floors (-) and is a function of the water depth and the inter-floor height of the building

IH is the inter-floor height (m)

BP is the basement perimeter (m)

BH is the basement height (m)

C is the damage (in EUR)

For some components, the damage is also calculated in terms of other intensity variables. For example, the replacement of partition walls is due to absorbed water that cannot be dried up. Damage occurs for long-lasting floods and, thus, has some proportionality to the duration of the flood. For more details about how the damage is computed for every component, the reader is referred to the original publication of the methodology (Dottori et al., 2016), as well as to its supplementary material.

In some cases, the vulnerability is modelled using probabilistic functions rather than deterministic ones. The probabilistic procedure considers the probabilities of occurrence of damage to the different components in order to obtain a distribution of the total building damage rather than a single value, enabling the treatment of uncertainties in the damage mechanisms considered in the model. Some examples of components treated with probabilistic functions are dehumidification, screed, pavement and baseboard removal and replacement, removal of partition walls, plaster removal, doors and windows removal and replacement, all the structural damage components, external and internal plaster replacement. For more information, the reader is referred to the original vulnerability model publication (Dottori et al., 2016).

The result is a set of vulnerability curves expressed in absolute terms (i.e., flood depth – or other variables – vs absolute damage in EUR). These curves can be combined in different ways, depending on the building categories included in the exposure database. In an ideal scenario of data availability, the buildings in the exposure database would be classified according to a large number of variables, such as number of floors, height of the ground floor over the street level and depth of the basement. Furthermore, the flood event would be characterised according to an array of variables, for example, flood depth, flow velocity and flood duration. However, this approach is not possible in a large-scale risk model covering five large countries with more than 75 million people. Certain approximations have to be made, because of the scale of the problem and because of the data available, resulting in a categorisation that has a granularity lower than ideal.

The strength of the component-based methodology is that, by combining the component-specific vulnerability curves, an “average” curve for any aggregated category can be obtained. For example, if the exposure classification does not consider explicitly the depth of the basement, this can be considered by deriving the empirical distribution of basement depths for each exposure category from data (for example: for masonry buildings, $x\%$ of the buildings have a one-floor basement, $y\%$ of the buildings have a two-floor basement and $z\%$ of the building have no basement) and computing a weighted sum of the corresponding vulnerability functions (e.g., weighting the one-floor basement curve by $x/100.$, the two-floor basement one by $y/100$ and the no basement one by $z/100$).

In this project, the aggregated variables not included in the exposure classification and therefore considered in a statistical way are:

- Number of floors (height of the building);
- Basement height;
- Ground floor level;
- Building type (apartment, detached, semi-detached).

Their weights are shown as follows. Data were collected from a variety of sources, cited below, including data collected during the exposure workshops conducted within the framework of the present project within Task 8 – Capacity Building and Knowledge Transfer and from experienced local advisors and engineers. Table 7 shows the weights for the aggregated variable “number of floors”. These weights have been derived mainly from Pittore et al. (2020) and Wieland et al. (2015), who defined ranges of floor numbers for each building categories based on local surveys (Figure 4). Other sources of data were KazNIISA (Kazakh Research and Design Institute of Construction and Architecture), with whom the consortium interacted in the early stages of the exposure development, Pittore et al. (2011) and The World Bank (2017) for Kyrgyz Republic, and a sample of 2538 buildings surveyed in Dushanbe (Tajikistan), also part of Pittore et al. (2020).

Table 7. Weights of the aggregated variable “number of floors” for each exposure category.

Exposure class	Number of floors							
	1	2	3	4	5	6	7	8
URM1	0	0.45	0.4	0.15	0	0	0	0
URM2	0.6	0.4	0	0	0	0	0	0
CM	0.4	0.4	0.1	0.05	0.05	0	0	0
RM-L	1	0	0	0	0	0	0	0
RM-M	0	0	1	0	0	0	0	0
RC1	0	0	0.3	0.3	0.2	0.1	0.1	0

Exposure class	Number of floors							
	1	2	3	4	5	6	7	8
RC2	0	0	0.3	0.3	0.2	0.1	0.1	0
RC3	0	0.45	0.4	0.15	0	0	0	0
RC4	0	0	0	0	0	0	0	1
RCPC1	0.2	0.2	0.15	0.15	0.1	0.1	0.05	0.05
RCPC2	0	0	0	0	0.4	0.3	0.2	0.1
ADO	1	0	0	0	0	0	0	0
WOOD1	0.6	0.4	0	0	0	0	0	0
WOOD2	0.6	0.4	0	0	0	0	0	0
STEEL	1	0	0	0	0	0	0	0
OTH	0.6	0.4	0	0	0	0	0	0
school	0.6	0.4	0	0	0	0	0	0
hospital	0.6	0.4	0	0	0	0	0	0
commercial	0.6	0.4	0	0	0	0	0	0
industrial	1	0	0	0	0	0	0	0

EMCA Type	Subtype	Building Class	Building Subclass	Country Code
EMCA-1	1.1	Load bearing masonry wall buildings	Unreinforced masonry, buildings with walls of brick masonry, stone, or blocks in cement or mixed mortar (no seismic design), wooden floors. Built between 1940 and 1955. 2–4 stories.	KY-1.4
			Unreinforced masonry, buildings with walls of brick masonry, stone, or blocks in cement or mixed mortar (no seismic design), precast concrete floors. Built since 1975. 1–2 stories.	KY-1.5
	1.3		Confined masonry. Built since 1960. 1–5 stories.	KY-1.6 KY-1.1
			Masonry with seismic provisions (e.g., seismic belts). Built between 1948 and 1959. 1–3 stories.	KY-1.2 KY-1.3
EMCA-2	2.1	Monolithic reinforced concrete buildings	Buildings with monolithic concrete moment frames. Built since 1950. 3–7 stories.	KY-2.1
			Buildings with monolithic concrete frame and shear walls (dual system). Built since 1987. 7–25 stories.	KY-2.2
			Buildings with monolithic concrete frames and brick infill walls. Built since 1975. 3–7 stories.	KY-2.3
			Buildings with monolithic reinforced concrete walls. Built since 1980. 8–16 stories.	KY-4
EMCA-3	3.1	Precast concrete buildings	Precast concrete large panel buildings with monolithic panel joints, Seria 105. Built since 1964. 1–16 stories.	KY-3.1
			Precast concrete large panel buildings with panel connections achieved by welding of embedment plates, Seria 464.	KY-3.2
			Precast concrete flat slab buildings (consisting of columns and slabs), Seria KUB. Built between 1980 and 1990. 5–9 stories.	KY-2.8
			Prefabricated reinforced concrete frame with linear elements with welded joints in the zone of maximum loads or with rigid walls in one direction, Seria 111, IIS-04. Built between 1966 and 1970. 6–7 stories.	KY-9.5
EMCA-4	4.1	Nonengineered earthen buildings	Buildings with adobe or earthen walls. Built since 1850. 1 story.	KY-9.5
EMCA-5	5.1	Wooden buildings	Buildings with load bearing braced wooden frames. Built between 1950 and 1970. 1–2 stories.	KY-9.7
			Building with a wooden frame and mud infill. 1–2 stories.	KY-9.6
EMCA-6	6	Steel buildings		KY-8

Figure 4 – Building types from (Wieland et al., 2015).

Table 8 shows the weights for the aggregated variable “basement height”.

Table 8. Weights of the aggregated variable “Basement height” for each exposure category.

Exposure class	Basement height (m)	
	0	3
URM1	0.75	0.25
URM2	0.75	0.25
CM	0.75	0.25
RM-L	0.75	0.25
RM-M	0.75	0.25
RC1	0.5	0.5
RC2	0.5	0.5
RC3	0.5	0.5
RC4	0.5	0.5
RCPC1	0.5	0.5
RCPC2	0.5	0.5
ADO	1	0
WOOD1	0.9	0.1
WOOD2	0.9	0.1
STEEL	0.75	0.25
OTH	0.5	0.5
school	0.5	0.5
hospital	0.9	0.1
commercial	0.5	0.5
industrial	0.9	0.1

Table 9 shows the weights for the aggregated variable “ground floor level”. Sample buildings from Google Maps images and other sources were also used to determine these weights.

Table 9. Weights of the aggregated variable “Ground floor level” for each exposure category.

Exposure class	Ground floor level (m)		
	-0.5	0	0.5
URM1	0.4	0.3	0.3
URM2	0.4	0.3	0.3
CM	0.4	0.3	0.3
RM-L	0.4	0.3	0.3
RM-M	0.4	0.3	0.3
RC1	0.4	0.3	0.3
RC2	0.4	0.3	0.3
RC3	0.4	0.3	0.3
RC4	0.4	0.3	0.3
RCPC1	0.4	0.3	0.3
RCPC2	0.4	0.3	0.3
ADO	0.4	0.3	0.3
WOOD1	0.4	0.3	0.3
WOOD2	0.4	0.3	0.3
STEEL	0.4	0.3	0.3
OTH	0.4	0.3	0.3
school	0	1	0
hospital	0	1	0
commercial	0	1	0
industrial	0	1	0

Table 10 shows the weights for the aggregated variable “building type”.

Table 10. Weights of the aggregated variable “Building type” for each exposure category.

Exposure class	Building type		
	Detached	Semi-detached	Apartment
URM1	0.4	0.4	0.2
URM2	0.4	0.4	0.2
CM	0.4	0.4	0.2
RM-L	0.4	0.4	0.2
RM-M	0.4	0.4	0.2
RC1	0.1	0.1	0.8
RC2	0.1	0.1	0.8
RC3	0.1	0.1	0.8
RC4	0.1	0.1	0.8
RCPC1	0.1	0.1	0.8
RCPC2	0.1	0.1	0.8
ADO	0.9	0.1	0
WOOD1	0.6	0.4	0
WOOD2	0.6	0.4	0
STEEL	0	0	1
OTH	0.8	0.2	0
school	1	0	0
hospital	1	0	0
commercial	1	0	0
industrial	1	0	0

Table 7, Table 8, Table 9 and Table 10 contain values that are inherently affected by uncertainty. This occurs because of the scale of the model: given that this risk model is a regional one, the taxonomy needs to be an aggregated one, i.e., every category contains buildings with different characteristics (for example, within the Reinforced Concrete class of buildings, some will have basements, some others will not, etc.). Furthermore, this uncertainty is also linked to the lack of very detailed data about these secondary building characteristics: number of storeys, basement height, ground floor level and building type.

While such uncertainty is unavoidable and will necessarily affect the final results, some comments can be made on how the final risk assessment will be affected. First of all, these four secondary characteristics can be ranked by their influence on the final vulnerability curves (this can be easily done through a simple sensitivity analysis, which was carried out within this project). The building type is certainly the least influential characteristic: it affects parameters such as the length of the external perimeter and in general has little effect on the final results. Basement height and ground floor level have a significant influence, because they dictate at which water depth the damage starts. It is reasonable to assume that the distribution of the ground floor levels is symmetrical with a median over 0 m above the street level, and as such has been treated in this project. The basement height is a characteristic that is difficult to estimate, given the absence of data. Within the inside model, the presence of a basement can alter the vulnerability of a building by up to 5% in correspondence with large flood events, i.e., for water depths larger than 2 m, the vulnerability of a building with a basement is typically larger than the one of a building with no basement by around 5% of the total replacement cost. Finally, the number of floors is the most influential building characteristic among the four ones listed here, since it heavily affects the total replacement cost.

However, data are available to estimate the distributions of number of storeys by category, such as Pittore et al. (2020) and Wieland et al. (2015), but also other data mentioned previously, and have been used in this project.

To use this methodological approach, we need to assume some of the buildings' characteristics. The model requires to specify the following building parameters: footprint area; external perimeter; inter-storey height; internal area; internal perimeter (considering partitions); basement area and basement perimeter.

In this project, the vulnerability curves have been developed for an archetype building with 100 m² footprint area, 40 m external perimeter, 90 m² internal area, 100 m internal perimeter, 3.5 inter-storey height, 50 m² basement area, 28 m basement perimeter. While the size of the archetype building obviously affects the absolute value of the damage (given a water depth level, the larger the building, the larger the damage), this has little or no influence on the final results of the vulnerability model, given that the final curves are normalised by the replacement cost of the building, which is also proportional to its size, i.e., they are provided as flood depth vs damage ratio (0-1) relationship.

These archetype building characteristics are in agreement with the representative buildings used in the literature for risk assessment in Central Asia, such as The World Bank (2017) (Figure 5 shows the distribution of the footprint areas, whose median is around 100 m², which is the value used in this project).

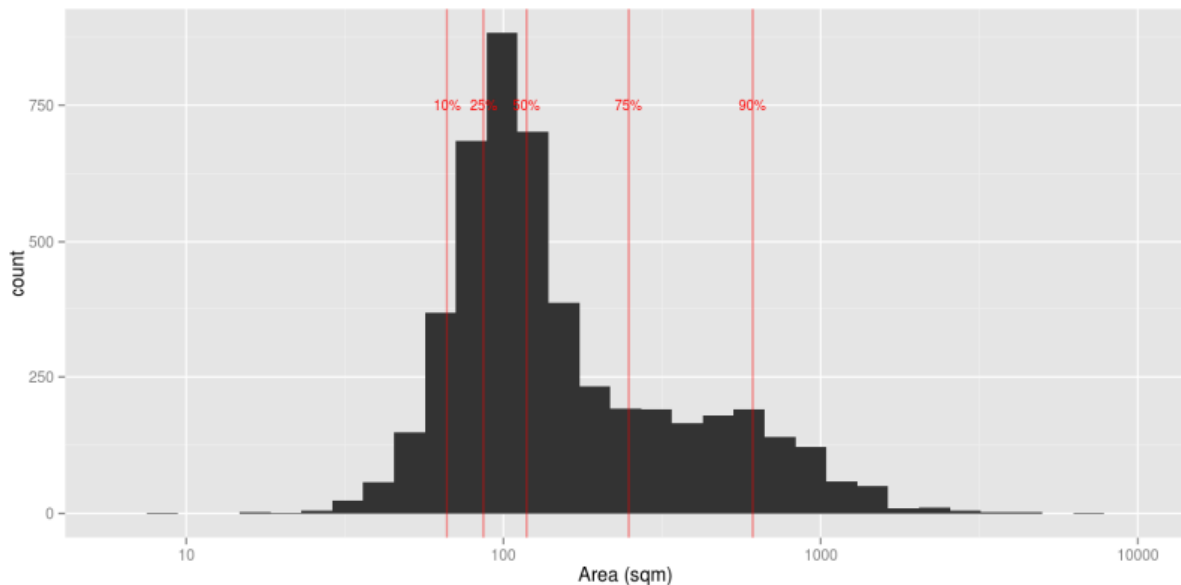


Figure 5 – Distribution of area of building footprints as derived from the OSM buildings dataset. Areas are in m² (The World Bank, 2017).

The component-based approach also requires unit costs for each component. These are the costs per unit (usually per m, m² or m³) of cleaning/removing/replacing each of the component. These costs have been collected onsite by local advisors and engineers through inquiries with engineers and architects involved in the design and pricing of buildings and from engineering manuals or real estate catalogues (for example, the ENiR - Uniform norms and prices for construction, installation and repairing works).

This piece of information is a key element of the vulnerability model, as it defines the costs repair/reconstruction of a building after a flood. Its importance relies not so much on the absolute values of these unit costs (as stated before, the vulnerability curves are normalised by the value of the building, and if the unit costs are high also the value of the building is high, and vice versa) but rather on the proportions among costs of components. For example, a country might have a low cost of labour but high cost of raw materials: in this case, the labour-intensive components will weigh less on the estimation of the total damage than the material-intensive components, altering the shape of the vulnerability curve. Another example is when a certain construction material is scarce or difficult to find (e.g., timber): in this case, the overall value of the building will be higher than that of buildings built with easier-to-find materials. Nevertheless, some components will have the same cost for both types of buildings (e.g., heating and electrical system, doors and windows), so when the curve is normalised by the total value, the high-cost building might have a lower vulnerability than the low-cost building

In the present project, different unit costs for each country have been estimated separately, to reproduce the differences in costs of repair/removal among countries. Data have also been homogenised to remove outliers and maintain a meaningful proportion between cost of components and the buildings' value. All costs have been converted from local currency to EUR. The values are shown in Table 11.

Table 11. Unit costs per country.

Category	Component	Kazakhstan	Kyrgyz Republic	Tajikistan	Turkmenistan	Uzbekistan	Unit
Clean-up	pumping water out of a basement/house	0.09	0.19	0.56	0.45	0.28	EUR/m ³
	removing and disposing debris and mud from a basement/house	1.20	2.62	3.55	6.28	19.75	EUR/m ³
	deep cleaning a house after a flood	0.83	6.39	0.89	0.43	0.24	EUR/m ²
	extracting humidity from walls and floors after a flood	0.17	0.37	1.33	0.90	0.71	EUR/m ³
Removal	removal of the screed	3.63	1.49	2.66	1.17	1.42	EUR/m ²
	removal of the wooden floor	1.91	0.78	1.40	0.62	0.75	EUR/m ²
	removal of the pavement/floor	1.63	1.52	3.25	1.34	1.98	EUR/m ²
	removal of the baseboard	0.08	0.08	0.17	0.07	0.10	EUR/m
	removal of internal walls/partitions	3.33	1.88	3.84	5.45	3.56	EUR/m ²
	removal of plasterboard	2.12	1.49	3.55	1.38	1.98	EUR/m ²
	removal of the external plaster	1.95	0.89	0.65	0.80	1.90	EUR/m ²
	removal of the internal plaster	1.95	0.89	0.65	0.80	1.58	EUR/m ²
	removal of the doors	3.81	2.66	1.63	4.19	3.95	EUR/m ²
	removal of the windows	3.44	2.66	1.63	4.19	3.95	EUR/m ²
removal of boiler	0.04	0.03	0.02	0.05	0.05	EUR/m ²	
Non-structural	construction of walls/internal partitions	13.45	3.81	8.27	50.27	9.01	EUR/m ²
	laying down the screed	3.74	2.43	2.81	3.77	2.77	EUR/m ²
	setting plasterboard	4.56	6.14	6.21	6.54	11.85	EUR/m ²
Structural	soil consolidation works	1.43	6.34	4.85	3.77	43.45	EUR/m ³

Category	Component	Kazakhstan	Kyrgyz Republic	Tajikistan	Turkmenistan	Uzbekistan	Unit
	local structural repair	7.50	4.63	5.61	5.39	4.74	EUR/m ²
	pillar retrofitting	39.05	39.48	15.37	45.96	67.15	EUR/m ²
Finishing	setting external plaster	1.68	5.89	3.14	5.86	3.95	EUR/m ²
	setting internal plaster	4.13	3.20	2.81	5.86	3.16	EUR/m ²
	external painting	1.93	3.19	2.26	4.19	3.56	EUR/m ²
	internal painting	1.52	2.70	1.92	4.19	3.24	EUR/m ²
	setting of the pavement	3.01	12.80	4.14	8.38	4.58	EUR/m ²
	replacing the baseboard	0.16	0.68	0.22	0.45	0.24	EUR/m
Windows and doors	replacement of doors	8.42	16.01	53.20	184.32	23.70	EUR/m ²
	replacement of windows	9.19	7.76	50.24	184.32	18.17	EUR/m ²
Building systems	replacement of the heating system	2.86	1.15	5.32	12.22	3.16	EUR/m ²
	painting the radiators	9.95	4.00	18.53	42.56	11.01	EUR
	replacement of the floor heating system	11.55	4.65	21.51	49.43	12.78	EUR/m ²
	replacement of the electrical system	6.88	3.78	9.16	29.45	5.14	EUR/m ²
	replacement of the plumbing system	4.64	2.54	7.98	19.84	4.35	EUR/m ²

As mentioned before, the resulting vulnerability curves are normalised by the total value of the building, which is derived by multiplying the cost per square metre of each category (intended as the cost per square metre of the whole building, not the cost per square metre of an apartment or of a single floor) by the external area of the archetype building. The costs per square metre for each category as well as the methodology for their estimation are shown in the Exposure report of the present project.

The unit cost approach allows building physically-based vulnerability curves, i.e., curves that are tailored over the actual costs of the buildings in a specific setting (i.e., in each of the five target countries). Furthermore, the normalisation by the total replacement cost allow factoring in the parts of the building that are not damageable (or very rarely damaged, such as the roof), since the total replacement cost include all components of a building rather than just the damageable ones.

As explained in the Introduction section, vulnerability curves were differentiated based on the local slope, considering the slope as a proxy for flood duration and flow velocity. In each of the three geomorphological areas (plains, hills and mountains), a distribution of the flood durations and flow velocities has been computed based on the results of the flood model developed in the Hazard module (see the report of Task 3 – Fluvial and Pluvial Flood hazard assessment) and some literature values (see for example Fox and Bryan, 2000). The resulting distributions are shown in Table 12.

Table 12. Flood duration and flow velocity distributions in each geomorphological area (plains have slower velocities and longer durations, mountains have faster velocities and shorter durations)

	Velocities (m/s)					Durations (h)		
	0.01	0.5	1	3	5	6	24	72
plains	30%	50%	15%	5%	0%	30%	50%	20%
hills	10%	40%	30%	20%	0%	70%	30%	0%
mountain	5%	10%	40%	40%	10%	90%	10%	0%

These distributions have allowed the production of three distinct vulnerability curves for each of the building categories shown in Table 1, by considering different values of flow velocity and flood duration. The result is that the vulnerability curves produced with this methodology are not only differentiated by country, but within each country they are differentiated by geomorphological area, i.e., similar assets will have different vulnerability curves depending on whether they are located in a plain, in a hilly area or in the mountains. In the plains the flood duration weights more than in the mountains, while in the mountains the flow velocity has a stronger influence than in the plains.

The methodology used to develop the vulnerability curves for buildings allows to reduce the uncertainty to a minimum, thanks to its physical basis. However, a certain level of uncertainty might still exist, and it is good practice when implementing a risk model to adjust the vulnerability curves based on comparisons between observed losses and modelled losses (either in probabilistic terms, e.g., exceedance probability curves, or on an event basis).

Bearing in mind the data availability limitations indicated above and the objective of the present study (which is to estimate the underlying, long-term average level of flood risk), the model calibration was carried out as follows:

1. A list of historical events and reported losses was collected;
2. The districts/regions affected by the historical floods were identified;
3. The risk model was run using the stochastic catalog of flood footprints as input, for all the district/regions identified previously;
4. The exceedance probability curves of all selected district/regions were calculated based on the results of the simulations with the stochastic catalog;
5. Based on the resulting exceedance probability curves, the return periods of the historical losses were computed (historical losses and district/region losses are comparable under the assumption that reported events are usually large floods that either affect the whole district/region or represent economic losses that are significant at the scale of the whole district/region);
6. The resulting return periods were critically analyzed under the following assumptions:
 - a. Reported events are typically large events that make the news, and therefore are relatively rare. It is expected that their return period is at least 5 years.
 - b. It is relatively unlikely that a reported flood event has a return period of more than 500-1,000 years.
 - c. If a region has more than one reported event, it is highly unlikely that all events have return periods longer than 100 years.
 - d. In general, it is expected that most reported floods have a return period between 5 and 100 years, with few outliers.
7. If some of the above criteria were not met, the vulnerability curves were adjusted to increase or decrease the losses and obtain a better adjustment to the criteria.

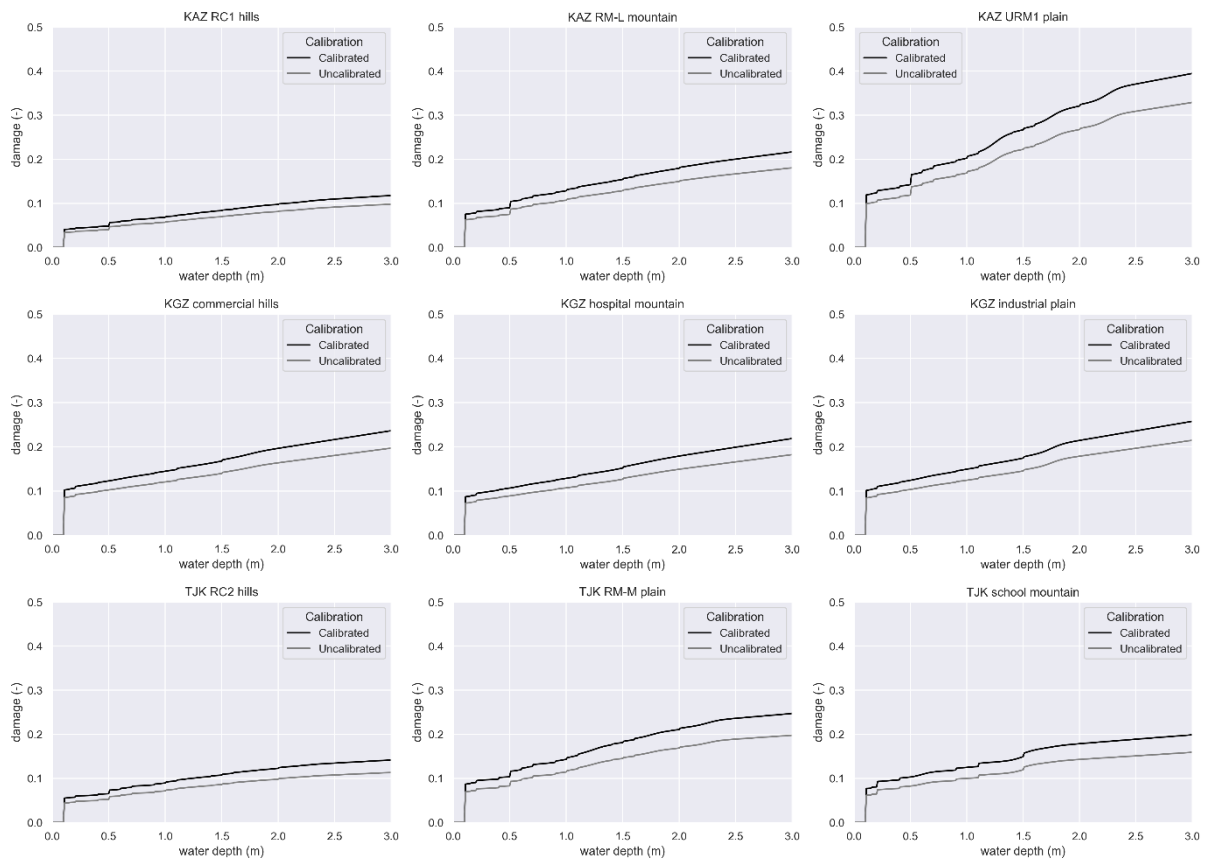
The rationale of this methodology is that, instead of providing direct comparisons between observed and reported losses (not possible given the available data), the calibration process tries to demonstrate that the model is providing risk estimates that are in line with what has been observed in the past 20 years in terms of frequency of the events and intensity of the economic losses. It is also the best possible attempt at exploiting all the data available.

Given the data limitation, and based on expert judgment, it was decided to reduce the number of calibration parameters to a minimum. Hence, all the curves were increased or decreased by the same amount, i.e., no differential calibration was carried out on vulnerability curves of different exposure classes or different countries. The results of the calibration for the flood vulnerability curves yielded an increase of the overall vulnerability of 20%.

In the Results section of this report, a comparison of calibrated and uncalibrated curves is provided for some taxonomy classes. Then, some calibrated curves are presented and discussed.

3.3 Results

Below, some examples of calibrated and uncalibrated vulnerability curves are shown, to provide an idea of the adjustments made to the relationships during the calibration phase.



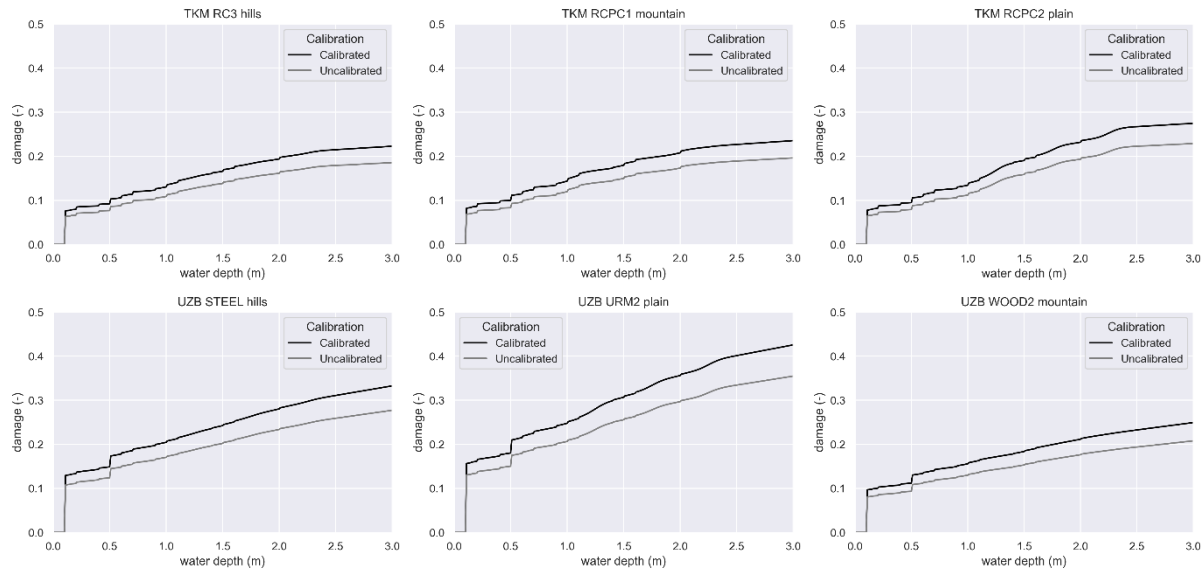


Figure 6 – Examples of calibrated vs uncalibrated vulnerability curves.

Some of the resulting vulnerability curves are shown as follows, grouped by category (see Table 1) and geomorphological area (Figure 7, Figure 8, Figure 9 and Figure 10). The ISO country codes used in the legend are:

- KAZ: Kazakhstan
- KGZ: Kyrgyz Republic
- TJK: Tajikistan
- TKM: Turkmenistan
- UZB: Uzbekistan

It is interesting to note that, while in general the countries have similar vulnerability rankings across all categories (e.g., Turkmenistan and Kyrgyz Republic are the most vulnerable countries and Kazakhstan and Uzbekistan the less vulnerable countries), an exception is represented by the category “WOOD1: Timber structure”, where Turkmenistan have a lower vulnerability compared to the other countries. This is due to the high cost of timber in Turkmenistan, where timber is considered a high-end construction material, compared to the rest of the Region. In particular, the low vulnerability is the result of the fact that a timber frame building in Turkmenistan has a relatively high replacement cost, due to the cost of the material, but the level of absolute damage such a building can experience due to a flood (especially a minor flood) is similar to other types of building (reinforced concrete, masonry), because the damaged components are essentially the same (paint, partitions, floor, etc.) and have very similar costs. Therefore, the same absolute damage divided by a higher replacement cost yields a lower relative vulnerability for timber frame buildings in Turkmenistan.

Another interesting feature is the presence of “steps” in the functions. These are due to the water depth reaching some features such as a window or the ceiling/floor of the first storey that cause the losses to increase suddenly.

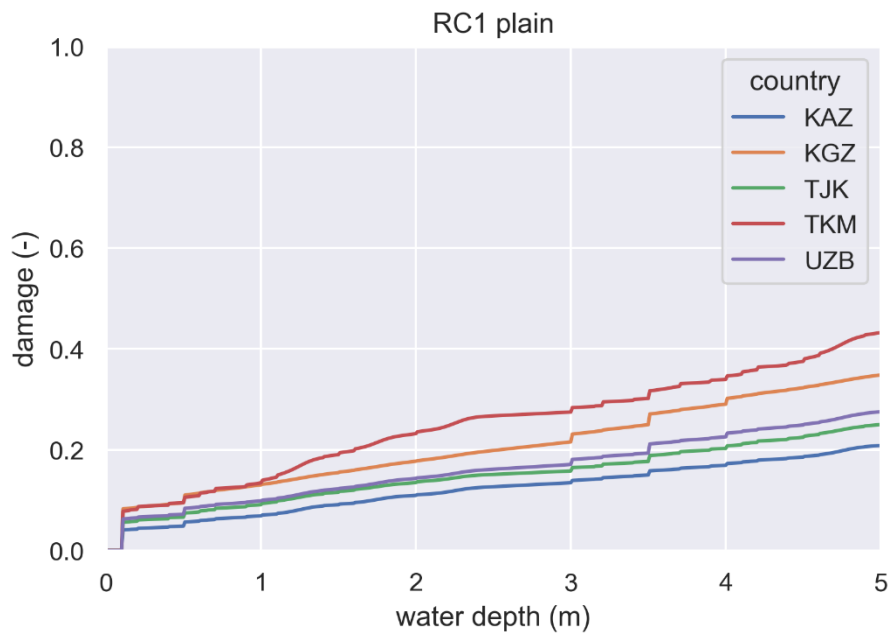


Figure 7 – Vulnerability curves for category “RC1: RC (reinforced concrete) frame without ERD” and geomorphological area “plains”.

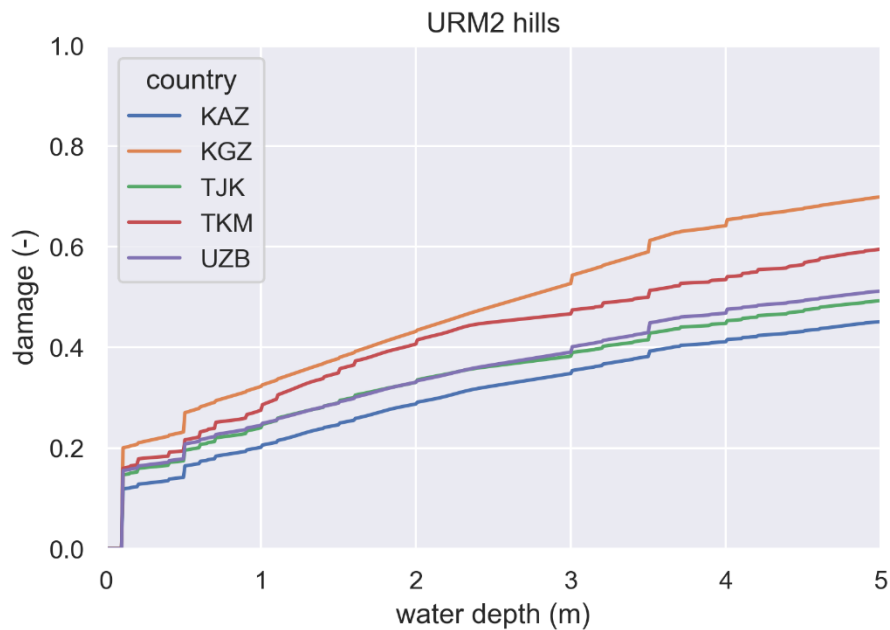


Figure 8 – Vulnerability curves for category “URM1: Unreinforced masonry” and geomorphological area “hills”.

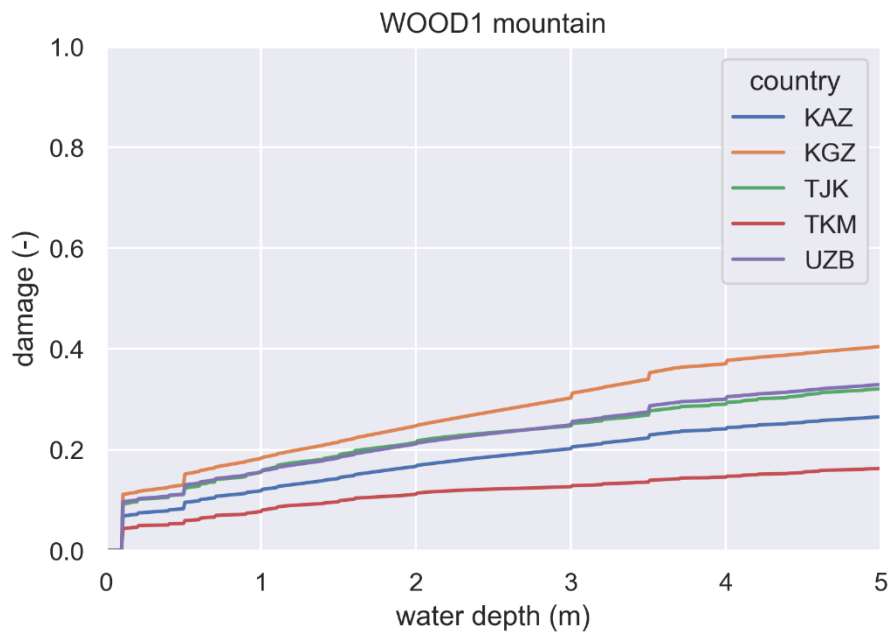


Figure 9 – Vulnerability curves for category “WOOD1: Timber structure” and geomorphological area “mountains”.

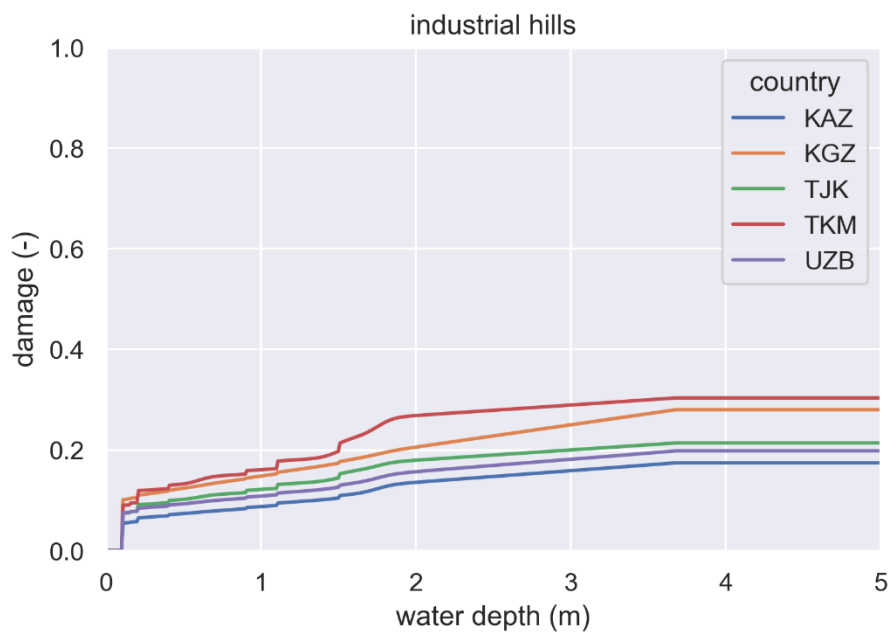


Figure 10 – Vulnerability curves for category “Industrial” and geomorphological area “hills”.

Figure 11 shows a comparison of vulnerability curves for the same country (Kazakhstan) and the same category (Unreinforced masonry) but different geomorphological areas (plains, hills and mountains). No large differences can be seen. However, it is worth noting that buildings located in plains are always the most vulnerable, due to the much longer flood durations, and that buildings located in the mountains have slightly larger vulnerability than building on hills, due to the faster flows.

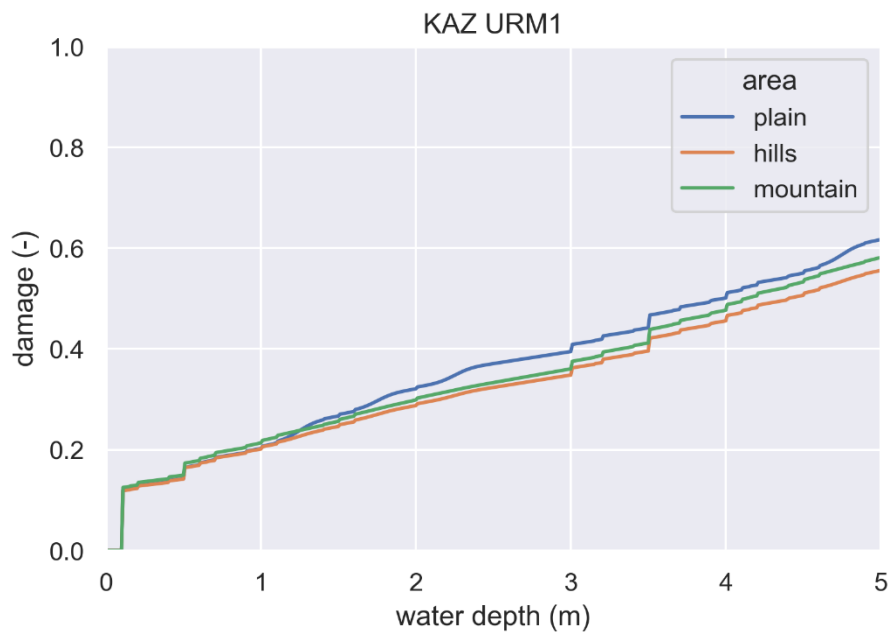


Figure 11 – Vulnerability curves for category “URM1: Unreinforced masonry” and geomorphological area.

For comparison purposes, Figure 12 shows the vulnerability curves residential, industrial and commercial buildings in Central Asia according to the Global Flood Depth-Damage database (Huizinga et al., 2017). GFDD curves are typically provided between 0 and 1, where 1 means maximum damage (that is, in these curves the damage ratio is defined as the fraction of the maximum damage, not of the total replacement cost). In order to compare these two sets of curves (GFDD and present project), GFDD damage ratios must be converted from "fraction of maximum damage" to "fraction of total replacement cost". To do so, and following the instructions of the GFDD manual, damage ratios must be first converted into actual damage values in USD, and this is done by multiplying them by national maximum damage values that are provided in a table. Then, normalised damage ratios can be calculated by dividing them by construction costs, which are also provided in a table as function of the GDP. This procedure was followed to obtain damage ratios expressed in terms of "fraction of total replacement cost", which are comparable with the curves presented in this report. GFDD curves are in agreement with the curves for masonry buildings developed in the present study (see for example Figure 8 and Figure 11), while they appear slightly above the curves developed in this project for reinforced concrete and wood (see for example Figure 7 and Figure 10). It must be noted that the curves developed in this project are expected to be more accurate, since they have been developed using data collected onsite and using more refined approaches than those by Huizinga et al. (2017). The objective of this comparison is not a strict validation (i.e., seeking perfect correspondence between the curves developed in this project and Huizinga et al., 2017) but rather a sanity check to verify that the magnitude of the damage is similar in both approaches, which is the case here.

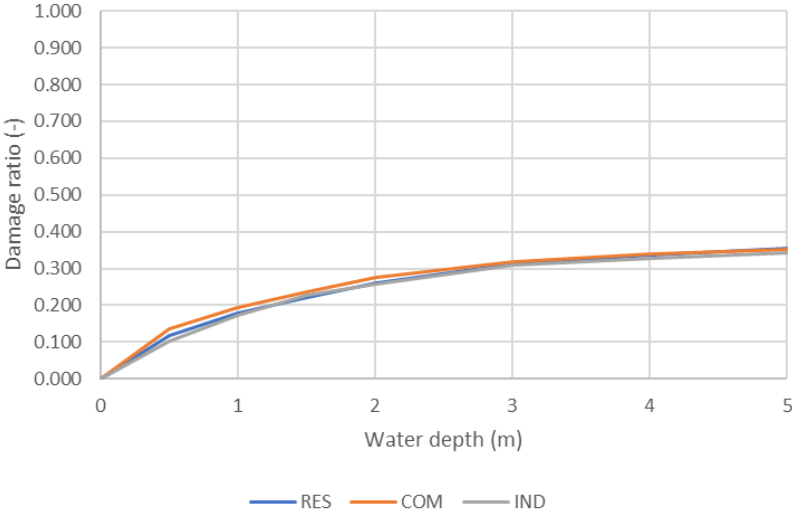


Figure 12 – Vulnerability curves residential, industrial and commercial buildings in Central Asia according to the Global Flood Depth-Damage database (Huizinga et al., 2017).

4 Infrastructure vulnerability

4.1 State of the art

Flooding poses an important threat to roads and can lead to massive disruption of traffic and cause damage to road structures, with possible long-term effects. At the same time, flooding leads to significant repair costs for road control authorities, and can generate access difficulties for emergency services (The World Bank, 2016). Given the focus of this project, which is targeted to evaluating direct damages by natural disasters, only the direct impact of floods on road (i.e., the economic losses due to repair and reconstruction) is considered.

Numerous studies have been conducted around the world to evaluate the vulnerability of roads to floods. In Europe, the Dutch Damage Scanner model (Klijn et al., 2007) is used frequently for road flood vulnerability (Figure 13), as well as the Dutch Standard Method (Kok et al., 2004) (Figure 14).

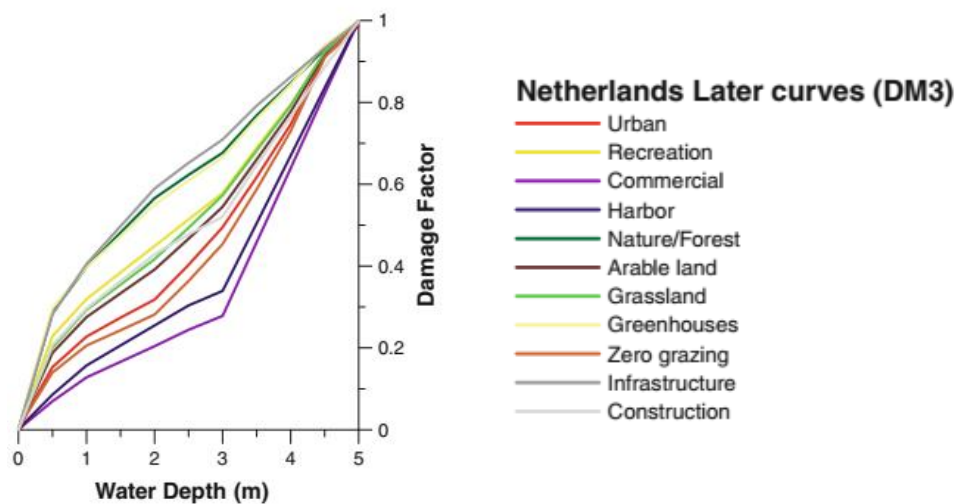


Figure 13 – Damage Scanner (Klijn et al., 2007) vulnerability curves, including infrastructure/road curve (Bubeck et al., 2011; de Moel and Aerts, 2011).

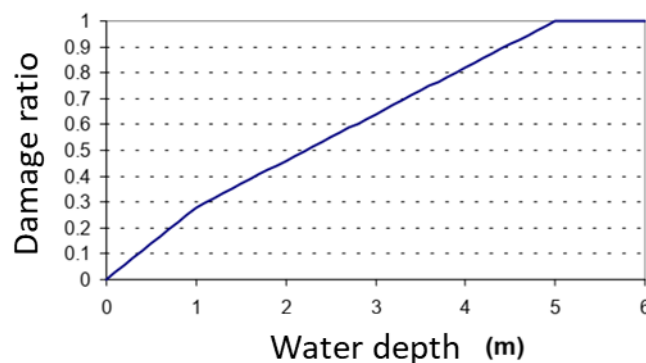


Figure 14 – Standard Method vulnerability curves for roads and railways (Kok et al., 2004).

A comprehensive analysis of the European road network vulnerability to flood was recently published (van Ginkel et al., 2021), where new object-based vulnerability curves were produced, as shown in Figure 15, as well as values of maximum damage and road construction costs.

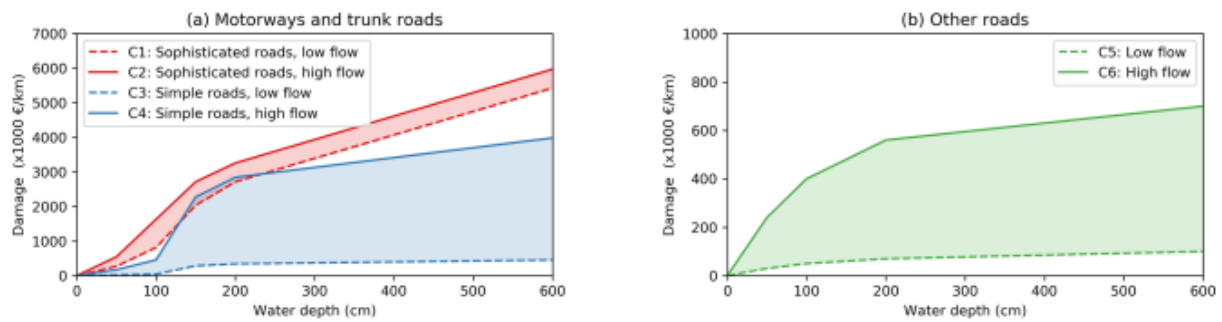


Figure 15 – Damage curves for illustrative values of road construction costs, in euros per kilometre (van Ginkel et al., 2021).

The literature is also rather rich for roads and infrastructure in the US (studies not cited here). However, not many flood vulnerability studies for roads in Central Asia, or in other parts of Asia for that matter, have been published. One example is Oddo et al. (2018), which derived vulnerability curves for roads in Vietnam and South East Asia.

The most common approach to model infrastructure vulnerability in areas where little or no information is available is the use of the Global Flood Depth-Damage curves (Huizinga et al., 2017). This dataset of vulnerability curves is a globally consistent database of depth-damage curves developed by the Joint Research Centre based on an extensive literature review. It provides normalised curves for all continents to guide flood risk assessment in countries where no damage model is currently available. Figure 16 shows the literature curves for Asia analysed in this database, as well as the average Asian and European curves.

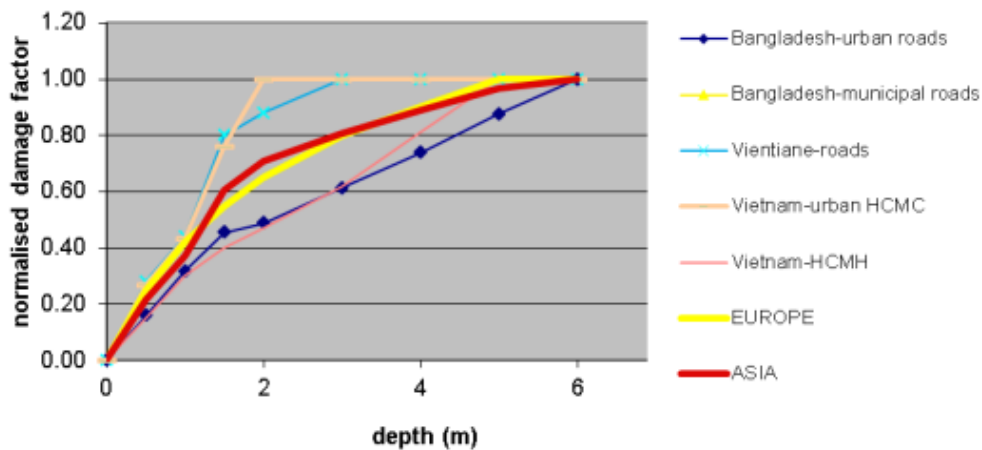


Figure 16 – Flood vulnerability curves for roads and infrastructure for Asian countries and comparison with the European curve (Huizinga et al., 2017).

Flood vulnerability curves for railways are in general much rarer in the literature and, despite the potential damage they can suffer from a flood, have received less attention compared to flood vulnerability of roads (Figure 17). Often, the same vulnerability curve used for roads is also assigned to railways, as in the Dutch Standard Method (Kok et al., 2004) and its updated version, the SSM2015 (de Bruijn et al., 2015). Kellermann et al. (2015) used the generic “infrastructure” curve from the Damage Scanner model (Klijn et al., 2007) for railways in Austria. Wang et al. (2021) adjusted the SSM2015 model to adapt it for countries other than the Netherlands (Figure 18).

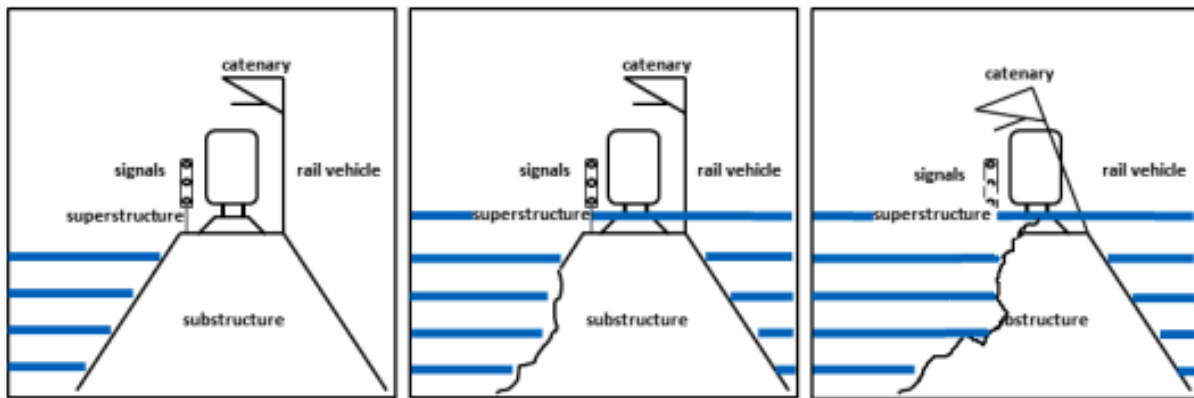


Figure 17 – Railway damage mechanisms (Kellermann et al., 2015).

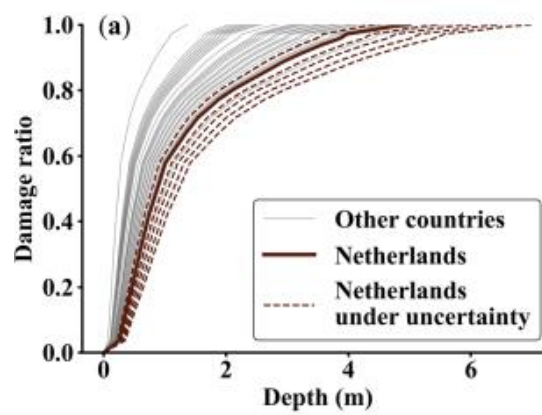


Figure 18 – Railway vulnerability curves for the Netherlands (de Bruijn et al., 2015) and for other countries (Wang et al., 2021).

No single specific vulnerability curve for airport exists in the literature. Normally, high-resolution flood vulnerability models for airports disaggregate damage into airport subcomponents (runway, terminal buildings, etc.).

4.2 Methodology

Given the lack of specific country-level vulnerability curves and the widespread level of acceptance within the risk modelling community of the Global Flood Depth-Damage curves' database, in this project the vulnerability for roads and railways will be modelled using the vulnerability curve for infrastructure/roads provided by Global Flood Depth-Damage database. More specifically, we will be using the curve provided for Asia. While this curve is dominated by South-East Asian data, it is also very similar to the curve for Europe, to which the road and railway systems of Central Asia share similarities.

Regarding airports, the vulnerability curve has been built by combining curves for different components (towers, runways, terminal, parking, fuel facilities, hangars, etc.), weighted by their cost normalised by the total cost of an average airport. The costs of the components have been taken from HAZUS (HAZard United States) (FEMA, 2018), the natural hazard analysis tool developed and freely distributed by the US Federal Emergency Management Agency (FEMA). They are shown in Figure 19. It is assumed that, while the absolute values of the component costs vary greatly from the US to the Central Asian countries, the proportions among components are

similar. Vulnerability curves for building-like components (terminal control towers, etc.) are assumed to be analogous to those of the reinforced concrete building vulnerability curves described in the previous section of this document, while the runway vulnerability curve is assumed to be analogous to that of the road curve.

Flood Label	General Occupancy	Specific Occupancy	Hazus Valuation ¹
ACTW	Airport Control Towers	Wood Airport Control Towers	5,000
ACTS	Airport Control Towers	Steel Airport Control Towers	5,000
ACTC	Airport Control Towers	Concrete Airport Control Towers	5,000
ACTB	Airport Control Towers	Brick Airport Control Towers	5,000
APTR	Airport Runway	Airport Runway (total)	28,000
AFF	Fuel Facilities	Fuel Facilities	5,000
AFO	Seaport/Stolport/Gliderport/etc.	Seaport/Stolport/Gliderport/etc.	500
AFH	Heliport Facilities	Heliport Facilities	2,000
APS	Airport Parking Structure	Airport Parking Structure	1,400
AMFW	Airport Maintenance & Hangar Facility	Wood Airport Maintenance & Hangar Facility	3,200
AMFS	Airport Maintenance & Hangar Facility	Steel Airport Maintenance & Hangar Facility	3,200
AMFC	Airport Maintenance & Hangar Facility	Concrete Airport Maintenance & Hangar Facility	3,200
AMFB	Airport Maintenance & Hangar Facility	Brick Airport Maintenance & Hangar Facility	3,200
ATBW	Airport Terminal Buildings	Wood Airport Terminal Buildings	8,000
ATBS	Airport Terminal Buildings	Steel Airport Terminal Buildings	8,000
ATBC	Airport Terminal Buildings	Concrete Airport Terminal Buildings	8,000
ATBB	Airport Terminal Buildings	Brick Airport Terminal Buildings	8,000
ATBU	Airport Terminal Unknown	Airport Terminal Buildings Unknown	8,000

Figure 19 – Costs of airport components (Scawthorn et al., 2006). Amounts in thousands of dollars.

Power supply and water supply facilities are assimilated to industrial buildings and included in the industrial category. Oil and gas pipelines and dams are considered not vulnerable to floods.

4.3 Results

Figure 20 shows the vulnerability curves for roads/railways and for airports developed in this project. Given the level of uncertainty and the lack of specific country-level data, no differentiation by country was considered (i.e., all countries are considered to have the same infrastructure vulnerability).

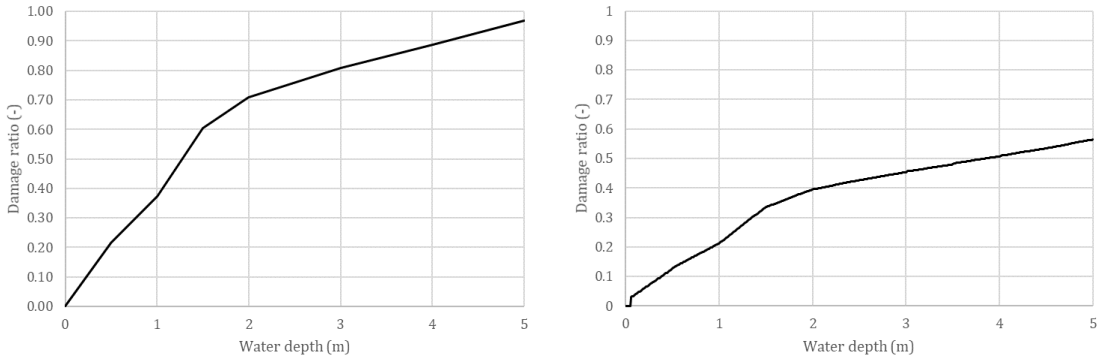


Figure 20 – Vulnerability curve for roads and railways (left) and for airports (right) used in this project (the road and railway curve is taken from the GFDD database, the airport curve is elaborated from GFDD and HAZUS).

5 Crop vulnerability

5.1 State of the art

A large number of crop-specific flood vulnerability studies were reviewed, especially those focusing on (but not limited to) studies in Asia and crops that can be found in the target countries. Some of these studies are summarised in Table 13.

Table 13. Studies on flood vulnerability of crops.

Reference	Geographical area	Crops
Baky et al., 2020	Bangladesh	rice
Forte et al., 2006	Italy	multiple
Hendrawan and Komori, 2021	Indonesia	rice
Rahman and Di, 2020	Global	multiple
Win et al., 2018	Myanmar	rice
Wu et al., 2016	China	multiple
Yazdi and Salehi Neyshabouri, 2012	Iran	fruit trees
Kwak et al., 2015	Cambodia	rice
Qian et al., 2020	China	cotton
Molinari et al., 2019	Italy	maize
Huizinga et al., 2017	Global	multiple

Some considerations can be drawn from this review:

- Depending on the level of detail of the study, vulnerability curves can be classified by type of crop (e.g., rice, cotton, and maize), by broad category of crops (e.g., cereals and fruit trees) or be lumped together in a single generic crop curve.
- The water depth is generally used as the intensity measure adopted for estimating damage, but the flood duration is also acknowledged to play a very important role as well.
- Depending on the level of detail of the study, seasonality can also be considered, i.e., different vulnerability curves are used for different growing seasons (for example, seedling, reproductive, vegetative, maturity), thus assuming that the response to a flood event of a crop varies depending on its vegetative state. For example, crops such as rice tend to be more vulnerable right after seedling, and less vulnerable once the plant has reached maturity.

As an example of the vulnerability curves found in the literature, Figure 21 shows all the flood vulnerability curves found for rice.

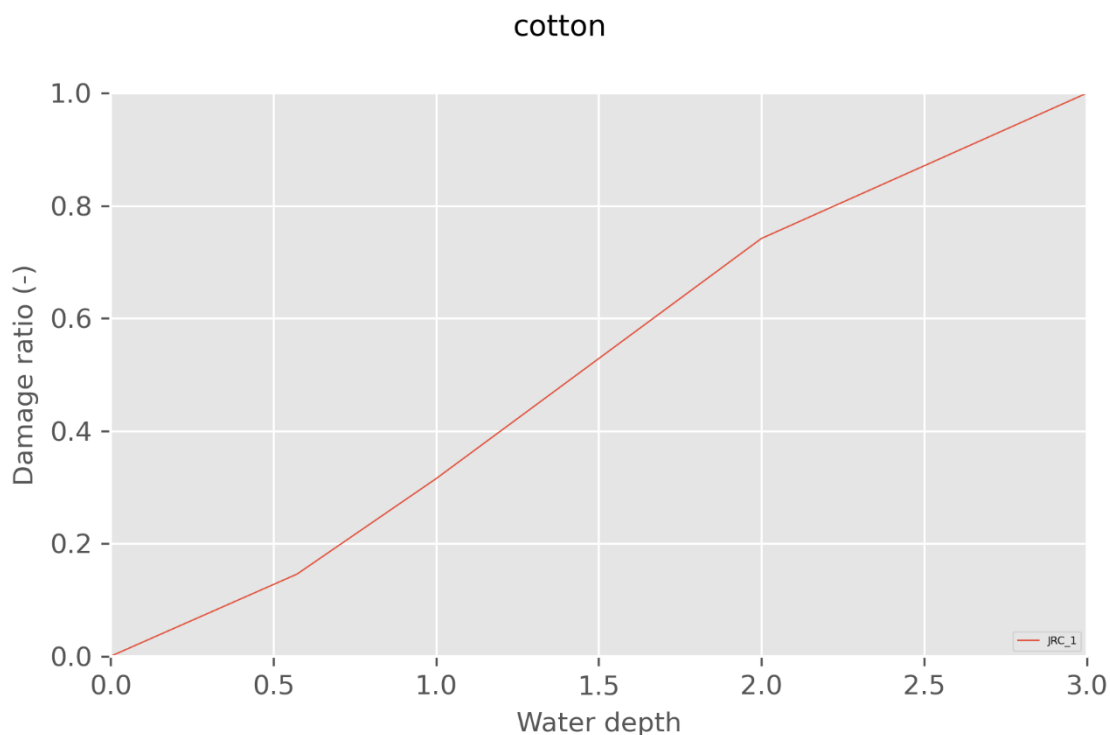


Figure 21 – Literature flood vulnerability curve for cotton.

5.2 Methodology

The most common cash crops in the target countries, according to the Water Use Efficiency Monitor in Central Asia platform, WUEMOCA (CAWA, 2019; Sychev and Mueller, 2018), are cotton, wheat, rice, alfalfa, vegetables, maize and sunflower. From an economic point of view, cotton and wheat are overwhelmingly the most relevant cash crops in the area. Considering also the scale and resolution of the present project, therefore, only cotton and wheat have been assigned a crop-specific vulnerability function, while a “generic” crop function is used for all the other exposed crops. The cotton curve has been derived as the average of the cotton vulnerability curves found in the literature. The wheat curve has been derived from similar crops (no specific wheat curves were found, but vulnerability curves for other cereals exist) and slightly adjusted based on agronomic considerations (i.e., considering similarities and differences with other crops that might make wheat more or less vulnerable compared to other crops). The “generic” curve has been derived as the average of a set of vulnerability curves for other types of crops.

As done for buildings and infrastructures, crop vulnerability curves have been expressed as relationships between water depth and damage ratio, where the damage ratio is the percentage of lost harvest due to floods. Damage ratio equals one when the average expected harvest is lost. However, acknowledging the importance of flood duration in the vulnerability of crops, three different vulnerability curves have been developed for every crop, each corresponding to a geomorphological area (plains, hills and mountains), similarly to what has been done for buildings (see Figure 1).

It is worth mentioning that most of the agricultural areas in the region are located in plains, in particular the areas where crops are cultivated for commercial purposes.

Low slope areas show larger losses compared to those on crops located on steeper terrains, due to the longer duration of floods. Studies from the literature, in particular Qian et al. (2020) have been used to quantify the effect of different flood durations.

Regarding crop seasonality, we made the conservative assumption that floods will always hit when crops are the most vulnerable, i.e., crop vulnerability curves are an upper bound of all seasonal curves for the same type of crop. The reason behind this simplification is that a flood risk model of this scale and geographical extension does not allow taking into account seasonality explicitly. This is because the uncertainty in the definition of the growing season is very high (they vary from year to year, from a climatic zone to another, they also depend on the irrigation regime, etc.) and using a seasonal approach to crop vulnerability would necessarily imply making several assumptions whose impact on the final results is unknown a priori. Given that no explicit seasonal approach can be used (e.g., different vulnerability curves for different seasons), a single curve for every crop has been developed, i.e., the vulnerability curve of the most vulnerable season.

5.3 Results

Figure 22 shows the vulnerability curves for crops developed in this project. No differentiation by country was considered (i.e., all countries are considered to have the same crop vulnerability).

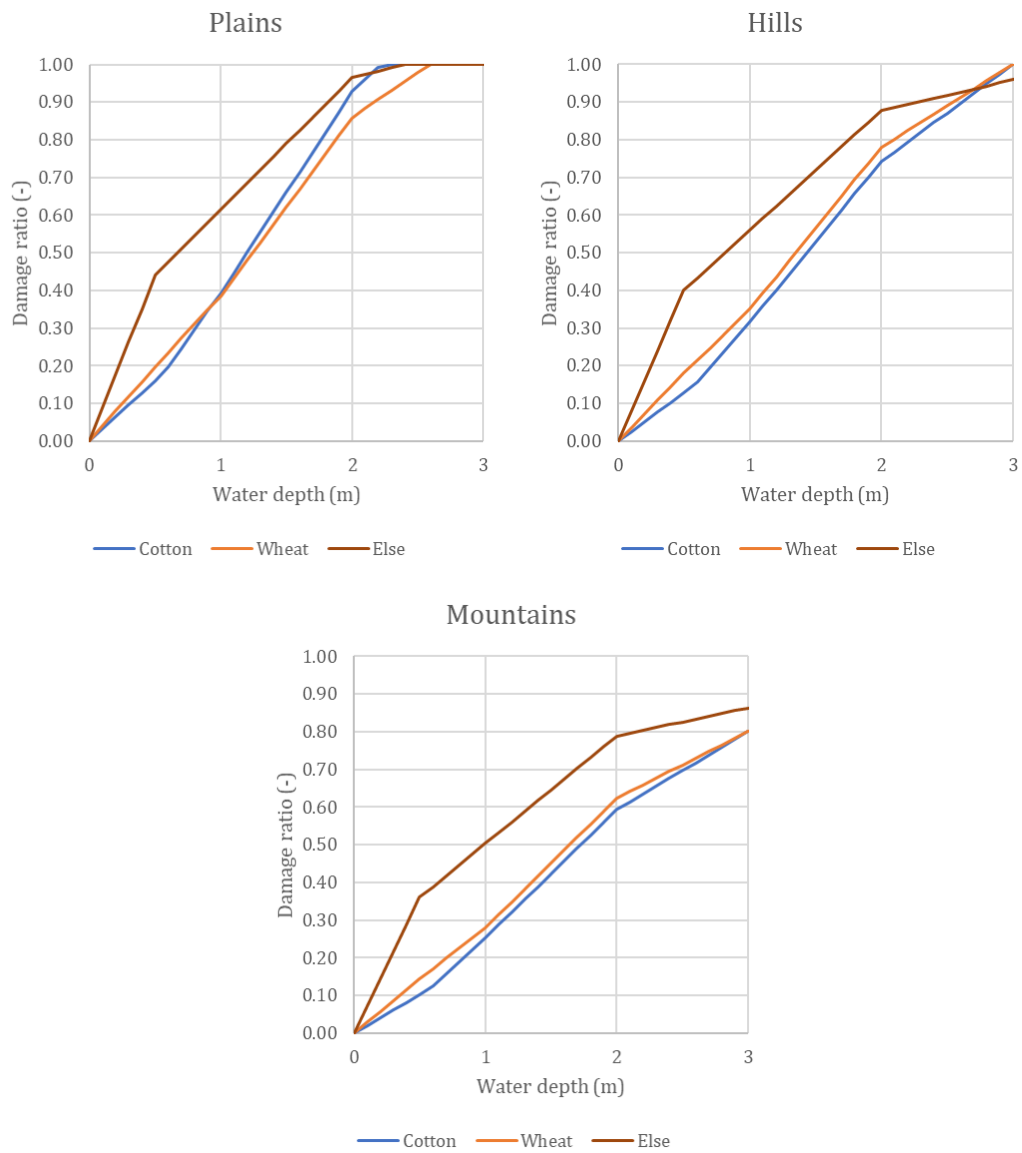


Figure 22 – Vulnerability curve for cash crops used in this project.

6 Human vulnerability

6.1 State of the art

Human safety in floods has been studied from a quantitative point of view since the 70s. Stability of humans with different height and mass combinations when subject to floods were studied in laboratory flumes and in real conditions by a range of studies that considered also different physical, emotional and dynamic factors. Conceptual models have also been introduced since the 90s, to describe the human stability as a function of flow velocity and water depth (Figure 23 shows a conceptual representation of a human body). The most frequent failure mechanisms to be found in the literature are slipping, toppling and drowning. Slipping limits stability in the range of high velocities and low depths, whilst toppling dominates in the range of high-water depths and low velocities. Drowning occurs when the water level reaches a maximum admissible threshold. The most relevant physical factors affecting human stability are water depth, flow velocity, local slope and fluid density.

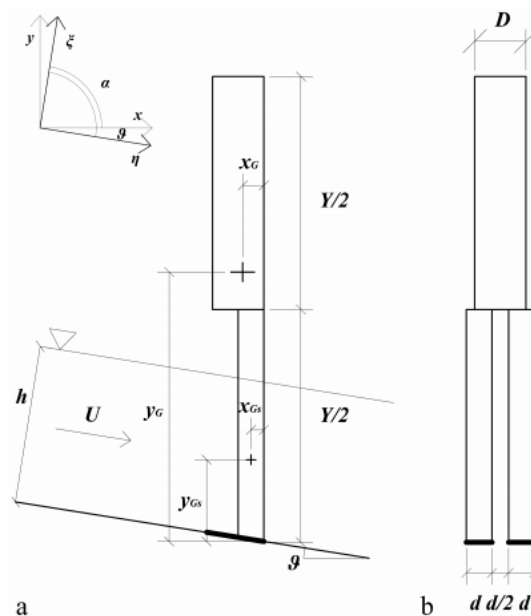


Figure 23 – Simplified representation of the human body in a (a) lateral and (b) frontal view (Milanesi et al., 2016).

Human stability models typically carry out a simple balance of forces to find whether failure occurs, according to any of the three mechanisms mentioned above, at a certain level of water, given certain conditions of flow velocity, debris, slope and body shape. Some examples are Jonkman and Penning-Rowsell (2008), Xia et al. (2014) and Milanesi et al. (2016).

6.2 Methodology

In this project, the methodology proposed by Milanesi et al. (2016) was used to establish the relationship between water depth and probability of failure depending on a person's gender and age. The human body is conceptualized as a set of cylinders and its stability to slipping and toppling is assessed by forces and moments equilibrium. Moreover, a depth threshold to consider drowning is assumed. The model also considers explicitly local slope, thus allowing for the characterisation

of vulnerability both in floodplains and in mountainous areas. The physical basis of the model allows to identify two stability thresholds, derived respectively for children and adults. No differentiation is made between adults and elderly, given that no assumptions regarding body strength are made within this model. For more information regarding the details of the model the reader is referred to Milanesi et al. (2016).

The parameterisation of the human bodies was based on a set of sources such as:

- World Data: <https://www.worlddata.info/average-bodyheight.php>
- Our World in Data: <https://ourworldindata.org/grapher/average-height-of-men-for-selected-countries?tab=table>
- Wikipedia: https://en.wikipedia.org/wiki/Average_human_height_by_country
- Baten and Blum (2014, 2012)

Body weight and height were introduced in the model in a probabilistic way, i.e., a Monte Carlo simulation of the model was conducted using multiple realisations of body weight and height extracted from pre-defined distributions based on the values retrieved in the sources cited above.

Three different vulnerability curves have been developed for every age and gender category, each corresponding to a geomorphological area (plains, hills and mountains), similarly to what has been done for buildings (see Figure 1) and crops (Figure 22).

Flow velocity in each geomorphological area was determined in a probabilistic manner, i.e., a Monte Carlo simulation of the model was conducted using multiple values of flow velocities extracted from flow velocity distributions obtained with simulations of the flood model for selected flood events (Figure 24).

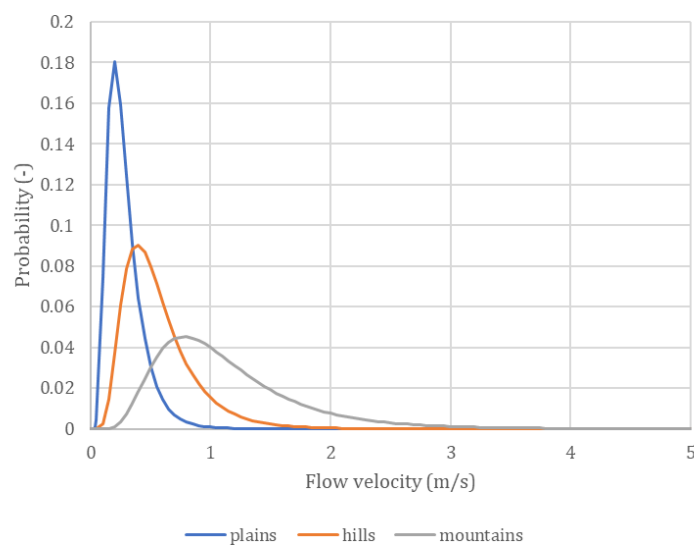


Figure 24 – Flow velocity distributions according to the geomorphological area.

The results of the methodology employed in this project provide a relationship between the water depth and the probability of failure in case a person is directly hit by a flood. However, it is safe to assume that not all the population of a flooded area will be directly hit by a flood. Some people might be elsewhere, for example to work or school, and people living at upper floors will not have the same probability of losing their lives than people living in the lower floors. For this reason, a coefficient of reduction, also called occupancy rate, needs to be introduced to account for such

factors. This coefficient is proportional to the average occupation of buildings and to the number of floors (assuming homogeneous distribution of people across all floors). For example, data like the ones provided by Pittore et al. (2011) for Kyrgyz Republic might assist in determine this coefficient (Figure 25). They seem to suggest an average number of floors between 3 and 5 (which would indicate that only between 20% and 50% of the persons might be at risk of losing their lives due to a flood), with rates of occupancy typically above 20%. According to these data, a reasonable range for the coefficient of reduction should be between 0.05 and 0.25, which is in agreement with reference values (Sarmah et al., 2020; Wang et al., 2020).

Other references, such as Feinberg et al. (2016) suggest that an upper bound of fatality rate (i.e., the fraction of people at risk that is projected to die, which is different from the occupancy rate discussed here) might be between 30% and 100% in cases of severe floods with no flood warning, but that this ratio should be lower (e.g., 15%) in case of medium severity floods. Other authors (Norkhairi et al., 2018; Sun et al., 2010) provide smaller values for medium severity floods, around 0.5-1%. However, in medium severity floods fatality rates are generally lower or much lower than occupancy rates, because most of the persons directly hit by the flood still survive. Jonkman et al. (2008) reviewed data from historical floods and found that, for a water depth of 2 m (which is a water depth for which the physical model employed here always return failure), fatality rate was between 0 and 15% for storm surges (thus, events with a warning of typically 1 or 2 days). However, they also suggested a very large dependency of the mortality rate from the length of the warning time. For slowly rising waters, such mortality rate for 2 m water depth decreases to 1%. Jonkman and Vrijling (2008) confirmed the 1% mortality rate for slowly rising coastal floods.

Housing Type	PAGE R Type	No. of Stories	No. of Units	Occupancy (family per unit)	Occupancy work hours	Occupancy night hours	Rural/ Urban	Inventory Description	EMS-98 (min -likely- max)
Precast reinforced concrete frame with cruciform and linear beam elements (series 106)	PC2H	9-12	60 (36-120 families per building)	1 / 2	> 20	> 20	Urban	Common in urban areas built after 1975	B-C-D
Single-family brick masonry house	UFB4	2	1	1	< 5	5-10	Both	Most common throughout the country	B-C-D
prefabricated concrete panel buildings with monolithic panel joints	PC1	5-9	60 (40-80)	1	> 20	> 20	Urban	About 35-40% of multistory building stock	D-E-F
Reinforced concrete frame buildings without beams (serie KUB)	PC2M	5-12	36 (10-120)	1	> 20	> 20	Urban	Exists in urban areas of the country	A-B-C
Buildings with cast-in-situ load-bearing reinforced concrete walls	CH2	4-18	54 (20-90 families per building)	1	> 20	> 20	Urban	Widespread in urban areas	D-E-F
Two-story unreinforced brick masonry building with wooden floors	UFB2	2	8-16	1	10-20	>20	Urban	5% of urban building stock	A-B-C
Houses with mud walls and thatch roofs	M2	1	1	1	< 5	5-10	Both	Common in the country	A-A-A

Figure 25 – Occupancy and number of floors for buildings in Kyrgyz Republic (Pittore et al., 2011).

While sometimes it is difficult to relate mortality and occupancy rates without a proper practical assessment of historical events, it appears that the spread of the values of this coefficient is rather high. For this reason, such coefficient was adjusted during the risk modelling phase, comparing the modelled fatalities with statistics of historical flood casualties in the target countries. A value of 0.01 was obtained.

6.3 Results

Figure 26, Figure 27, Figure 28, Figure 29 and Figure 30 show the flood vulnerability curves for human beings, developed in this project (assuming a coefficient of reduction equal to 0.01). Curves are differentiated by countries (i.e., for the same gender and age, curves of different countries differ among each other). This differentiation is based on national height and weight statistics, which change country by country. Obviously, the differences are small, as reflected in the results. For example, with 1 m of water in a plain area, female child vulnerability is 0.89 in Kazakhstan, 0.95 in Kyrgyzstan, 0.95 in Tajikistan, 0.93 in Turkmenistan and 0.97 in Uzbekistan.

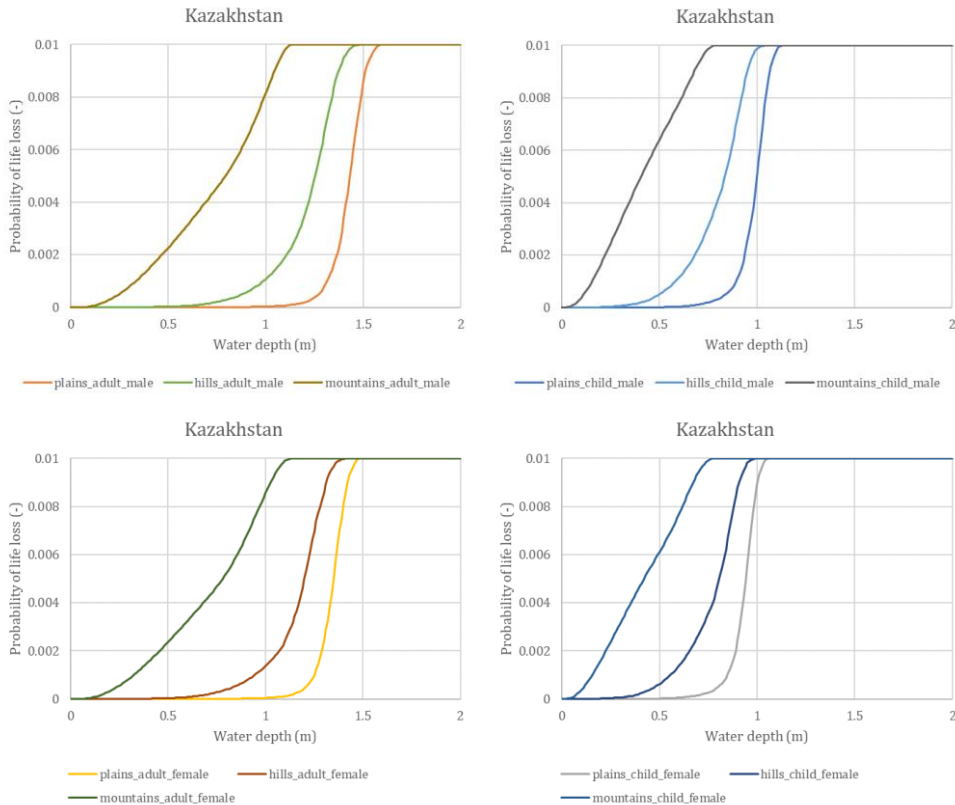


Figure 26 – Vulnerability curve for human beings used in this project (Kazakhstan).

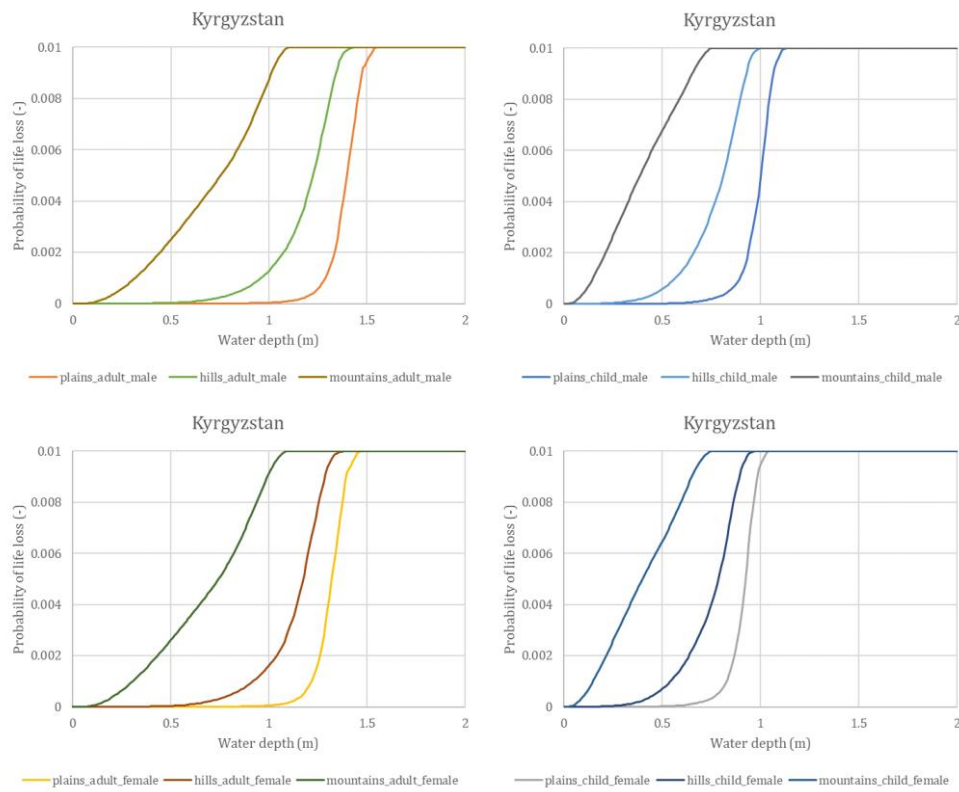


Figure 27 – Flood vulnerability curve for human beings used in this project (Kyrgyz Republic).

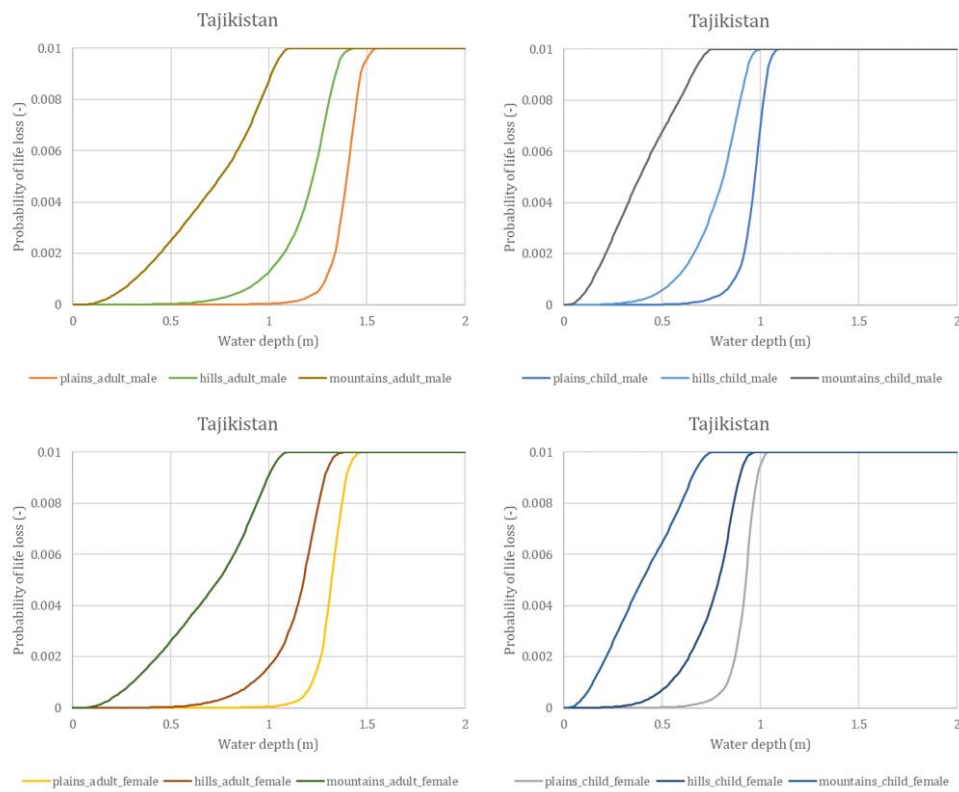


Figure 28 – Flood vulnerability curve for human beings used in this project (Tajikistan).

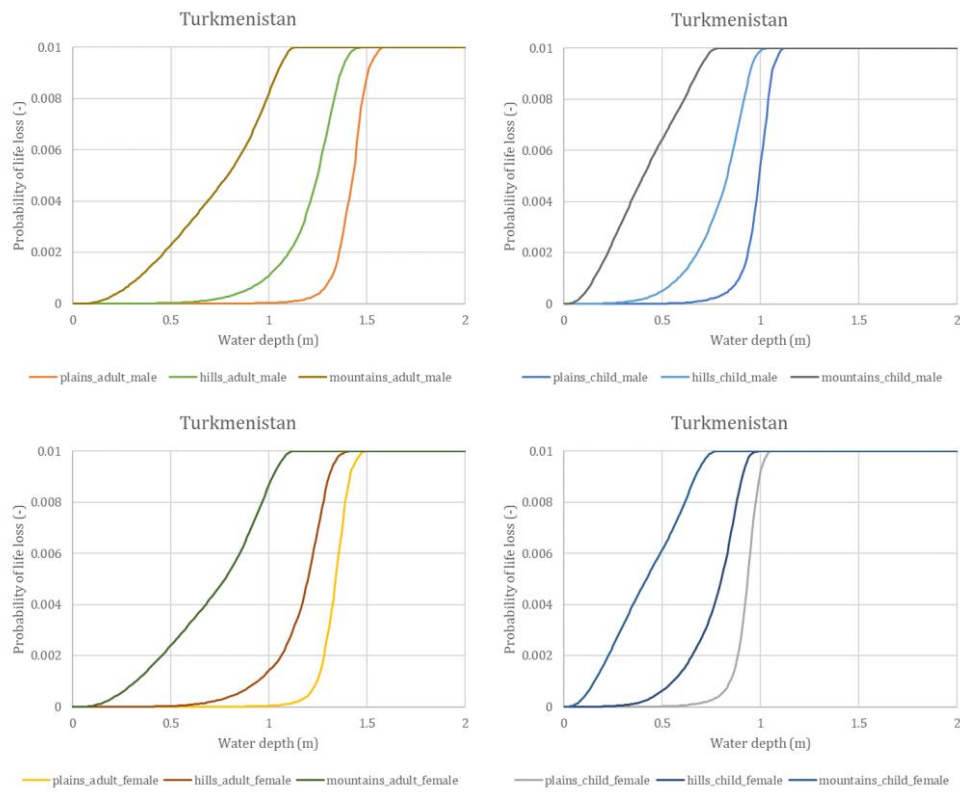


Figure 29 – Flood vulnerability curve for human beings used in this project (Turkmenistan).

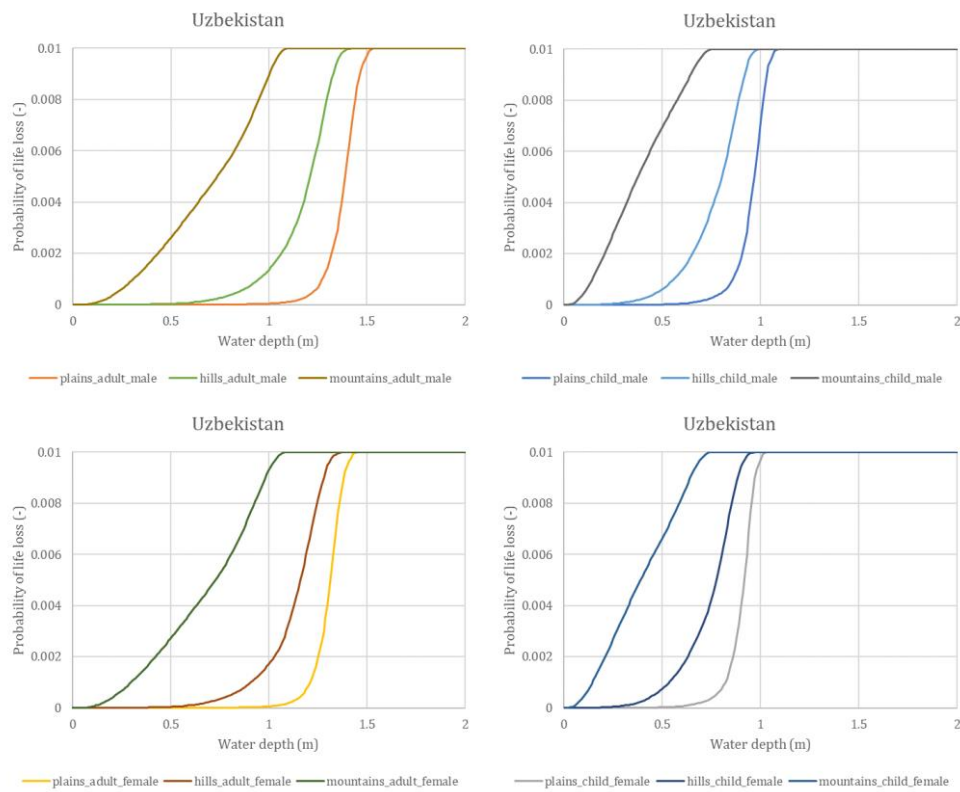


Figure 30 – Flood vulnerability curve for human beings used in this project (Uzbekistan).

7 Conclusions

This report shows the methodology followed for the development of flood vulnerability curves for five Central Asia countries (Kazakhstan, Kyrgyz Republic, Tajikistan, Turkmenistan and Uzbekistan). This vulnerability module is part of a flood risk model developed within the framework of a European Union- and World Bank-funded project called “SFRARR Central Asia disaster risk assessment” (*Regionally consistent risk assessment for earthquakes and floods and selective landslide scenario analysis for strengthening financial resilience and accelerating risk reduction in Central Asia*).

These curves define the response of a set of assets to floods, measured in terms of economic losses or life loss. The assets considered in this project are grouped in four categories: buildings (residential, commercial, industrial and schools), infrastructure (roads, railways and airports), cash crops and population. When possible, curves have been differentiated for geomorphological areas, i.e., different curves have been developed for plains hills and mountains, based on the local slope, to account for the effect of flow velocity and flood duration on the flood damage.

While the methodology followed in the development of the flood vulnerability model is sound and in agreement with the state of the art for regional disaster risk assessment, some limitations can be identified, with the aim of defining areas for future improvement. First, data limitations can be mentioned, in particular regarding damage data. Damage data, i.e., accurate damage assessment on a building-by-building basis after major historical events is absent or not accessible in the five target countries. Should these data be collected after future events, they will provide an invaluable source of information of the development and/or validation of vulnerability curves. The implementation of systematic post-event damage surveys would certainly have a beneficial effect on the accuracy of any risk assessment based on the data collected. Another data limitation worth mentioning is the lack of data on the presence of basement, even at a statistical level (i.e., percentages of building with and without basement per city or per oblast), which is more related to exposure development, but has also a strong influence on flood vulnerability. From a methodological point of view, the procedure followed to develop vulnerability curves for buildings is the most accurate and up-to-date (although it would certainly benefit from more accurate data on component costs and total building costs), while infrastructure and crop vulnerability curves were developed based on literature curves, which can certainly be improved if specific vulnerability studies on local infrastructure and crops are carried out.

This flood vulnerability model will be coupled to a specific flood hazard model and to an exposure database covering the five target countries, with the aim of assessing economic risk and life loss risk caused by floods. The development and results of the whole risk model will be presented in a separate, specific report.

References

- Baky, M.A. Al, Islam, M., Paul, S., 2020. Flood Hazard, Vulnerability and Risk Assessment for Different Land Use Classes Using a Flow Model. *Earth Syst. Environ.* 4, 225–244. <https://doi.org/10.1007/s41748-019-00141-w>
- Baten, J., Blum, M., 2014. Why are you tall while others are short? Agricultural production and other proximate determinants of global heights. *Eur. Rev. Econ. Hist.* 18, 144–165.
- Baten, J., Blum, M., 2012. Growing tall but unequal: new findings and new background evidence on anthropometric welfare in 156 countries, 1810–1989. *Econ. Hist. Dev. Reg.* 27, S66–S85.
- Bubeck, P., de Moel, H., Bouwer, L.M., Aerts, J.C.J.H., 2011. How reliable are projections of future flood damage? *Nat. Hazards Earth Syst. Sci.* 11, 3293–3306. <https://doi.org/10.5194/nhess-11-3293-2011>
- CAWA, 2019. WUEMOCA: Informed Decision-Making in Land and Water Resources Management.
- de Bruijn, K., Wagenaar, D., Slager, K., de Bel, M., Burzel, A., 2015. Updated and improved method for flood damage assessment: SSM2015 (version 2). Deltares.
- de Moel, H., Aerts, J.C.J.H., 2011. Effect of uncertainty in land use, damage models and inundation depth on flood damage estimates. *Nat. Hazards* 58, 407–425. <https://doi.org/10.1007/s11069-010-9675-6>
- Dottori, F., Figueiredo, R., Martina, M.L.V., Molinari, D., Scorzini, A.R., 2016. INSYDE: a synthetic, probabilistic flood damage model based on explicit cost analysis. *Nat. Hazards Earth Syst. Sci.* 16, 2577–2591. <https://doi.org/10.5194/nhess-16-2577-2016>
- Feinberg, B., Engemoen, W., Fiedler, W., Osmun, D., 2016. Reclamation's Empirical Method for Estimating Life Loss Due to Dam Failure. *E3S Web Conf.* 7, 06002. <https://doi.org/10.1051/e3sconf/20160706002>
- FEMA, 2018. Hazus Flood Model User Guidance.
- Forte, F., Strobl, R.O., Pennetta, L., 2006. A methodology using GIS, aerial photos and remote sensing for loss estimation and flood vulnerability analysis in the Supersano-Ruffano-Nociglia Graben, southern Italy. *Environ. Geol.* 50, 581–594. <https://doi.org/10.1007/s00254-006-0234-0>
- Fox, D.M., Bryan, R.B., 2000. The relationship of soil loss by interrill erosion to slope gradient. *CATENA* 38, 211–222. [https://doi.org/10.1016/S0341-8162\(99\)00072-7](https://doi.org/10.1016/S0341-8162(99)00072-7)
- Hendrawan, V.S.A., Komori, D., 2021. Developing flood vulnerability curve for rice crop using remote sensing and hydrodynamic modeling. *Int. J. Disaster Risk Reduct.* 54, 102058. <https://doi.org/10.1016/j.ijdrr.2021.102058>
- Huizinga, J., de Moel, H., Szewczyk, W., 2017. Global flood depth-damage functions: Methodology and the database with guidelines. No. JRC105688. Joint Research Centre.
- Jonkman, S.N., Penning-Rowsell, E., 2008. Human Instability in Flood Flows 1. *JAWRA J. Am. Water Resour. Assoc.* 44, 1208–1218. <https://doi.org/10.1111/j.1752-1688.2008.00217.x>
- Jonkman, S.N., Vrijling, J.K., 2008. Loss of life due to floods. *J. Flood Risk Manag.* 1, 43–56. <https://doi.org/10.1111/j.1753-318X.2008.00006.x>
- Jonkman, S.N., Vrijling, J.K., Vrouwenvelder, A.C.W.M., 2008. Methods for the estimation of loss of life due to floods: a literature review and a proposal for a new method. *Nat. Hazards* 46, 353–389. <https://doi.org/10.1007/s11069-008-9227-5>
- Kellermann, P., Schöbel, A., Kundela, G., Thieken, A.H., 2015. Estimating flood damage to railway infrastructure – the case study of the March River flood in 2006 at the Austrian Northern Railway. *Nat. Hazards Earth Syst. Sci.* 15, 2485–2496. <https://doi.org/10.5194/nhess-15-2485-2015>
- Klijn, F., De Bruijn, K., Kwadijk, J., 2007. Overstromingsrisico's in Nederland in een veranderd klimaat. Verwachtingen, schattingen en berekeningen voor het project Nederland Later. Delft Hydraulics.

- Kok, M., Huizinga, H., Vrouwenfelder, A., Barendregt, A., 2004. Standard method 2004. Damage and casualties caused by flooding, Highway and Hydraulic Engineering Department.
- Kreibich, H., Piroth, K., Seifert, I., Maiwald, H., Kunert, U., Schwarz, J., Merz, B., Thielen, A.H., 2009. Is flow velocity a significant parameter in flood damage modelling? *Nat. Hazards Earth Syst. Sci.* 9, 1679–1692. <https://doi.org/10.5194/nhess-9-1679-2009>
- Kwak, Y., Shrestha, B.B., Yorozuya, A., Sawano, H., 2015. Rapid Damage Assessment of Rice Crop After Large-Scale Flood in the Cambodian Floodplain Using Temporal Spatial Data. *IEEE J. Sel. Top. Appl. Earth Obs. Remote Sens.* 8, 3700–3709. <https://doi.org/10.1109/JSTARS.2015.2440439>
- Luino, F., Cirio, C.G., Biddoccu, M., Agangi, A., Giulietto, W., Godone, F., Nigrelli, G., 2009. Application of a model to the evaluation of flood damage. *Geoinformatica* 13, 339–353. <https://doi.org/10.1007/s10707-008-0070-3>
- Milanesi, L., Pilotti, M., Bacchi, B., 2016. Using web-based observations to identify thresholds of a person's stability in a flow. *Water Resour. Res.* 52, 7793–7805. <https://doi.org/10.1002/2016WR019182>
- Molinari, D., Scorzini, A.R., Gallazzi, A., Ballio, F., 2019. AGRIDE-c, a conceptual model for the estimation of flood damage to crops: development and implementation. *Nat. Hazards Earth Syst. Sci.* 19, 2565–2582. <https://doi.org/10.5194/nhess-19-2565-2019>
- Norkhairi, F.F., Thiruchelvam, S., Hasini, H., 2018. Review Methods for Estimating Loss of Life from Floods due to Dam Failure. *Int. J. Eng. Technol.* 7, 93. <https://doi.org/10.14419/ijet.v7i4.35.22334>
- Oddo, P., Ahamed, A., Bolten, J., 2018. Socioeconomic Impact Evaluation for Near Real-Time Flood Detection in the Lower Mekong River Basin. *Hydrology* 5, 23. <https://doi.org/10.3390/hydrology5020023>
- Oliveri, E., Santoro, M., 2000. Estimation of urban structural flood damages: the case study of Palermo. *Urban Water* 2, 223–234. [https://doi.org/10.1016/S1462-0758\(00\)00062-5](https://doi.org/10.1016/S1462-0758(00)00062-5)
- Pittore, M., Bindi, D., Tyagunov, S., Wieland, M., Picozzi, M., Pilz, M., Ullah, S., Fleming, K., Parolai, S., Zschau, J., Moldobekov, B., Abdrakhmatov, K., Begaliev, U., Yasunov, P., Ishuk, A., Mikhailova, N., 2011. Seismic hazard and risk in Central Asia. Scientific Technical Report STR11/14. GFZ Helmholtz-Zentrum Potsdam. <https://doi.org/https://doi.org/10.2312/GFZ.b103-11149>
- Pittore, Massimiliano, Haas, M., Silva, V., 2020. Variable resolution probabilistic modeling of residential exposure and vulnerability for risk applications. *Earthq. Spectra* 36, 321–344. <https://doi.org/10.1177/8755293020951582>
- Pittore, M, M, H., Silva, V., 2020. Multi-resolution probabilistic modelling of residential exposure and vulnerability for seismic risk applications. *Earthq. Spectra.* <https://doi.org/10.1177/8755293020951582>
- Qian, L., Chen, X., Wang, X., Huang, S., Luo, Y., 2020. The Effects of Flood, Drought, and Flood Followed by Drought on Yield in Cotton. *Agronomy* 10, 555. <https://doi.org/10.3390/agronomy10040555>
- Rahman, M.S., Di, L., 2020. A Systematic Review on Case Studies of Remote-Sensing-Based Flood Crop Loss Assessment. *Agriculture* 10, 131. <https://doi.org/10.3390/agriculture10040131>
- Sarmah, T., Das, S., Narendr, A., Aithal, B.H., 2020. Assessing human vulnerability to urban flood hazard using the analytic hierarchy process and geographic information system. *Int. J. Disaster Risk Reduct.* 50, 101659. <https://doi.org/10.1016/j.ijdrr.2020.101659>
- Scawthorn, C., Flores, P., Blais, N., Seligson, H., Tate, E., Chang, S., Mifflin, E., Thomas, W., Murphy, J., Jones, C., Lawrence, M., 2006. HAZUS-MH Flood Loss Estimation Methodology. II. Damage and Loss Assessment. *Nat. Hazards Rev.* 7, 72–81. [https://doi.org/10.1061/\(ASCE\)1527-6988\(2006\)7:2\(72\)](https://doi.org/10.1061/(ASCE)1527-6988(2006)7:2(72))
- Sun, Y., Zhong, D., Li, M., Li, Y., 2010. Theory and application of loss of life risk analysis for dam break. *Trans. Tianjin Univ.* 16, 383–387. <https://doi.org/10.1007/s12209-010-1470-7>

- Sychev, V., Mueller, L., 2018. Optimising Agricultural Landscapes, in: Novel Methods and Results of Landscape Research in Europe, Central Asia and Siberia. Russian Academy of Science, Moscow.
- The World Bank, 2017. Measuring seismic risk in Kyrgyz Republic : seismic risk reduction strategy: Working Paper123049.
- The World Bank, 2016. Flood Risk in Road Networks. Technical Note.
- van Ginkel, K.C.H., Dottori, F., Alfieri, L., Feyen, L., Koks, E.E., 2021. Flood risk assessment of the European road network. *Nat. Hazards Earth Syst. Sci.* 21, 1011–1027. <https://doi.org/10.5194/nhess-21-1011-2021>
- Wang, G., Hu, Z., Liu, Y., Zhang, G., Liu, J., Lyu, Y., Gu, Y., Huang, X., Zhang, Q., Tong, Z., Hong, C., Liu, L., 2020. Impact of Expansion Pattern of Built-Up Land in Floodplains on Flood Vulnerability: A Case Study in the North China Plain Area. *Remote Sens.* 12, 3172. <https://doi.org/10.3390/rs12193172>
- Wang, Q., Liu, K., Wang, M., Koks, E.E., 2021. A River Flood and Earthquake Risk Assessment of Railway Assets along the Belt and Road. *Int. J. Disaster Risk Sci.* 12, 553–567. <https://doi.org/10.1007/s13753-021-00358-2>
- Wieland, M., Pittore, M., Parolai, S., Begaliev, U., Yasunov, P., Tyagunov, S., Moldobekov, B., Saidiy, S., Ilyasov, I., Abakanov, T., 2015. A Multiscale Exposure Model for Seismic Risk Assessment in Central Asia. *Seismol. Res. Lett.* 86, 210–222. <https://doi.org/10.1785/0220140130>
- Win, S., Zin, W.W., Kawasaki, A., San, Z.M.L.T., 2018. Establishment of flood damage function models: A case study in the Bago River Basin, Myanmar. *Int. J. Disaster Risk Reduct.* 28, 688–700. <https://doi.org/10.1016/j.ijdrr.2018.01.030>
- Wu, X., Zhou, L., Gao, G., Guo, J., Ji, Z., 2016. Urban flood depth-economic loss curves and their amendment based on resilience: evidence from Lizhong Town in Lixia River and Houbai Town in Jurong River of China. *Nat. Hazards* 82, 1981–2000. <https://doi.org/10.1007/s11069-016-2281-5>
- Xia, J., Falconer, R.A., Wang, Y., Xiao, X., 2014. New criterion for the stability of a human body in floodwaters. *J. Hydraul. Res.* 52, 93–104. <https://doi.org/10.1080/00221686.2013.875073>
- Yamazaki, D., Ikeshima, D., Sosa, J., Bates, P.D., Allen, G., Pavelsky, T., 2019. MERIT Hydro: A high-resolution global hydrography map based on latest topography datasets. *Water Resour. Res.* 2019WR024873. <https://doi.org/10.1029/2019WR024873>
- Yazdi, J., Salehi Neyshabouri, S.A.A., 2012. Optimal design of flood-control multi-reservoir system on a watershed scale. *Nat. Hazards* 63, 629–646. <https://doi.org/10.1007/s11069-012-0169-6>

Appendix A - List of acronyms

CAWA: Central Asian Water

EMCA: Earthquake Model of Central Asia

ERD: Earthquake-Resistant Design

EUR: Euro

FEMA: Federal Emergency Management Agency

GDP: Gross Domestic Product

GFDD: Global Flood Depth-Damage database

IS: Institute of Seismology

ISASUZ: Institute of Seismology of the Academy of Science of Uzbekistan

ISNASKR: Institute of Seismology of Kyrgyz Republic

ISO: International Organization for Standardization

IWPHE: Institute of Water Problems, Hydropower Engineering and Ecology

KAZ: Kazakhstan

KGZ: Kyrgyz Republic

MERIT: Multi-Error-Removed Improved-Terrain DEM

OSM: Open Street Map

RC: Reinforced Concrete

SFRARR: Strengthening Financial Resilience and Accelerating Risk Reduction in Central Asia

TJK: Tajikistan

TKM: Turkmenistan

US: United States

USD: United States Dollar

UZB: Uzbekistan

WUEMOCA: Water Use Efficiency Monitor in Central Asia platform